

EVALUATING WEARABLES FOR BEHAVIORAL STATE
MONITORING IN SEIZURE PATIENTS

Jal Mahendra Panchal

A THESIS

in

Robotics

Presented to the Faculties of the University of Pennsylvania

in

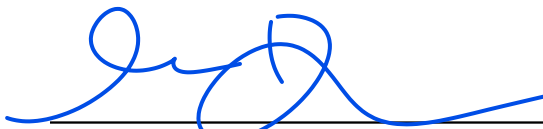
Partial Fulfillment of the Requirements for the

Degree of Master of Science in Engineering

2022

Brian Litt, MD

Dr. Brian Litt, Professor of Neurology, Neurosurgery and Bioengineering
Supervisor of Thesis



*Dr. Michelle Johnson, Associate Professor of Physical Medicine and Rehabilitation,
Mechanical Engineering, and Bioengineering*
Co-Supervisor of Thesis



*Dr. M. Ani Hsieh, Associate Professor of Mechanical Engineering and Applied
Mechanics*
Graduate Program Chair, ROBO

To my parents and family who make it all worthwhile

ACKNOWLEDGEMENT

I would first like to thank my mentors Dr. Brian Litt and Dr. Michelle Johnson who have believed in me and helped me grow into a researcher over the past couple years. I am also very grateful to the member of the Litt Lab and CNT lab, Brittany Scheid, Akash Pattnaik and the Pioneer team. I am also very thankful for the training and support provided by Dr. Lorenzo Caciagli as I tried to understand the world of network neuroscience. I also owe my success to the Rehabilitation Robotics Lab, for providing me the initial platform to explore research at Robotics and at Penn. I am also very appreciative of the support provided by the GRASP community through my time here.

Finally, I am truly grateful to my family and friends who have been the pillar of support throughout my life.

TABLE OF CONTENTS

ACKNOWLEDGEMENT	iii
LIST OF TABLES	vi
LIST OF FIGURES	vii
CHAPTER 1 : INTRODUCTION	1
1.1 Motivation	1
1.2 Research goals	2
1.3 Contributions	3
1.4 Summary of remaining chapters	3
CHAPTER 2 : WEARABLE DEVICES AND MEASUREMENTS	4
2.1 Measurements from Wearable devices	4
2.2 Heart rate parameters	5
CHAPTER 3 : PART I : NETWORK NEUROSCIENCE	7
3.1 Motivation	7
3.2 Methods	8
3.3 Results	11
3.4 Discussion	13
3.5 Conclusion	15
CHAPTER 4 : PART II : WEARABLE DEVICES AND BEHAVIORAL STATE DETECTION	17
4.1 Overview	17
4.2 Study Design	17
4.3 Trial Data Collection	18
4.4 Signal Processing	20

4.5 Results	21
4.6 Discussion	31
4.7 Conclusion	34
CHAPTER 5 : CONCLUSION	35
APPENDICES	37
BIBLIOGRAPHY	43

LIST OF TABLES

TABLE 4.1	Features of selected wearable devices	18
TABLE 4.2	Data streams from clinical trial	19
TABLE 4.3	Patients summary	22
TABLE A.1	Patient details for Part I : Network Analysis	37

LIST OF FIGURES

FIGURE 2.1 Wearable devices for seizure management	4
FIGURE 3.1 Steps in calculation of temporal changes in HRV and network properties	9
FIGURE 3.2 Node clustering using flexibility	10
FIGURE 3.3 Summary of correlation between HRV parameters and network parameters across all subjects	12
FIGURE 4.1 Clinical trial data streams	19
FIGURE 4.2 ECG signal processing	21
FIGURE 4.3 Overview of HR data collected and HRV calculations	23
FIGURE 4.4 Comparison of heart rate sampling	24
FIGURE 4.5 ECG vs Watch comparing HR and HRV values for all subjects . . .	25
FIGURE 4.6 ECG vs Watch comparing individual Subjects : Heart Rate	27
FIGURE 4.7 ECG vs Watch comparing individual Subjects : RMSSD	27
FIGURE 4.8 ECG vs Watch comparing individual Subjects : High frequency power	27
FIGURE 4.9 HRV stages : LB3_001_phaseII	29
FIGURE 4.10 HRV stages : LB3_004_phaseI	30
FIGURE 4.11 HRV stages : LB3_005_phaseII	32
FIGURE C.1 Node-wise core-periphery grouping changes and HRV parameters over time windows.	39
FIGURE C.2 Flexibility distribution of core-periphery group changes of network nodes.	40
FIGURE C.3 Correlation of HRV parameters with network parameter of all nodes and clustered nodes	41
FIGURE C.4 Selection of optimal γ	42

CHAPTER 1

INTRODUCTION

1.1. Motivation

Epilepsy is a disorder of the brain characterized by repeated seizures. A seizure is usually defined as a sudden alteration of behavior due to a temporary change in the electrical functioning of the brain. Normally, the brain continuously generates tiny electrical impulses in an orderly pattern. In epilepsy, the brain's electrical rhythms have a tendency to become imbalanced, resulting in recurrent seizures. In patients with seizures, the normal electrical pattern is disrupted by sudden and synchronized bursts of electrical energy that may briefly affect their consciousness, movements or sensations.

Seizures belong to one of two basic categories: primary generalized seizures and partial focal seizures. Primary generalized seizures typically begin with a widespread electrical discharge that involves both sides of the brain at once. Partial focal seizures begin with an electrical discharge in one limited area of the brain [1, 2]. About two-thirds of newly diagnosed epilepsies are partial and/or secondary generalized [3].

Seizures can last from a few seconds to a few minutes. They can have many symptoms, from convulsions and loss of consciousness to more subtle symptoms like blank staring, lip smacking, or jerking movements of arms and legs. Some symptoms of seizures are not always recognized as seizures by the person experiencing them or by health care professionals [4]. Diagnosis of epilepsy is dependent on history, physical and neurologic examination, laboratory testing as indicated, and electroencephalography and neuro-imaging findings [2].

Although there is no cure for epilepsy, there are many treatment options. Anti-epileptic drugs (AED) have shown to prevent seizures in the majority of people who take them regularly, with at least fifty percent of all patients with epilepsy gaining complete control of their seizures for substantial periods of time [5]. But about one-third of patients experience no

relief from AEDs and need additional treatment options [6]. Other treatment options for epilepsy include Vagus nerve stimulation, diet control and surgery. The goal of all epilepsy treatment is to prevent further seizures, avoid side effects, and make it possible for people to lead active lives [5].

Seizures are known to be unpredictable and people often struggle to identify triggers that start a seizure [7]. Most common trigger factors reported by people with epilepsy include emotional stress, sleep deprivation, and missing medications [8, 9]. The recognition and understanding of seizure triggers (ictogenic factors) or risk factors for the development of epilepsy (epileptogenic factors) therefore is of great interest to many patients [10]. Recent studies using postictal reporting and wearables devices have shown stress to be the most commonly reported seizure trigger often combined with one or more other triggers like lack of sleep and menses [9].

The physiological stress response is mediated by the neuro-endocrine system. The two main components of the response are the hypothalamic-pituitary-adrenocortical (HPA) axis and the sympathetic adrenomedullary (SAM) system [11]. The SAM system responds to stress via the two branches of the autonomic nervous system (ANS): the sympathetic and the parasympathetic nervous system (SNS and PNS). Previous studies have indicated that seizures have a tendency of activating sympathetic nervous activity, and that parasympathetic activation may be prominent during partial seizures [12, 13, 14]. Information about ANS activity can also be obtained from cardiac activity, in specific heart rate (HR) and heart rate variability (HRV) analysis. Prior research [15] has shown the presence of high HR or ictal tachycardia before seizure onset. Recent studies have also shed light on changes in network connectivity before seizures and the presence of changing brain states in the pre-ictal period [12].

1.2. Research goals

1. In Part 1 we explore the connection between ANS activity and temporal changes in functional connectivity of the brain before a seizure. We hypothesize that functional

connectivity of specific brain regions is associated more strongly with HRV changes and by extension with ANS activity than other brain regions.

2. In Part 2 we explore the use of 2 commercially available wearable devices: a Fitbit Sense and an Apple Watch Series 7 to identify behavioral state changes before and after seizures.

1.3. Contributions

In this study we make the following contributions:

1. Demonstrate the use of network neuroscience to find an association between temporal changes in functional connectivity of the brain and changes in heart rate parameters before a seizure.
2. Evaluate two commercially available wearable devices for continuous monitoring of HR and their use for people with epilepsy. We identify the strengths and weaknesses of the devices and offer suggestions to improve data collection and signal quality.
3. Present a method to compute behavioral state changes before and after a seizure using heart rate variability parameters.

1.4. Summary of remaining chapters

In Chapter 2 we provide an overview of wearable devices for biomonitoring and seizure management currently being used. We also list useful HRV parameters to measure behavioral changes and ANS activity. In Chapter 3 we demonstrate a method of finding the association between ANS activity and changes in the functional connectivity of the brain before a seizure. In Chapter 4 we evaluate two commercially available wearable devices, Fitbit Sense and Apple Watch Series 7, for continuous monitoring of HR. We also demonstrate a method to compute behavioral state changes, using heart rate variability parameters, before and after a seizure. In Chapter 5 we present concluding remarks and next steps.

CHAPTER 2

WEARABLE DEVICES AND MEASUREMENTS

2.1. Measurements from Wearable devices

Wearable devices are smart electronic devices that are worn close to and/or on the surface of the skin, where they detect, analyze, and transmit information concerning e.g. body signals such as vital signs, and/or ambient data and which allow in some cases immediate biofeedback to the wearer [16]. Wearable devices enable multi-modal sensing 24x7 allowing for continuous long-term monitoring of vitals. Wearable devices can provide valuable monitoring options for people with epilepsy including Electroencephalography (EEG), Electrocardiography (ECG), Electromyography (EMG), Electro dermal activity (EDA), skin temperature, accelerometry, sleep tracking, respiration rate, and exercise tracking.

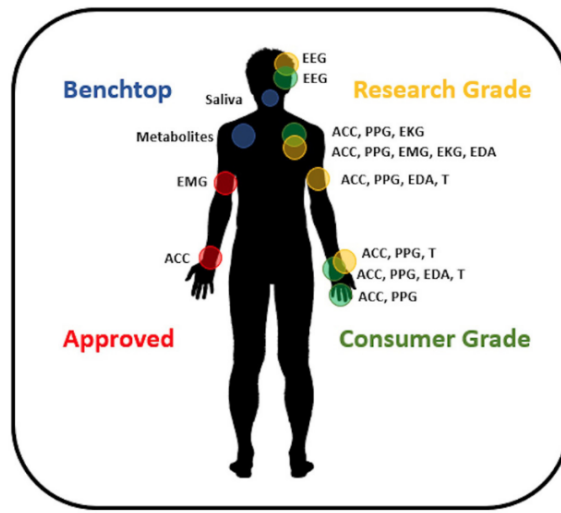


Figure 2.1: Available wearable devices for seizure management. Approved devices include sensor systems CE Marked and/or FDA approved for epilepsy. Research grade devices are commercially available and provide accurate, high-quality data. Consumer grade devices are commercially available sensors designed around applications where data accuracy is not crucial and may utilize interpolation or estimation methods to provide information to the user. Benchtop devices are innovative sensors under development and not available commercially. EEG, electroencephalography; ACC, accelerometry; PPG, photoplethysmography; EKG, electrocardiography; EMG, electromyography; EDA, electrodermal activity; T, temperature. Source: [17]

There are several commercially available wearable devices for monitoring different body vitals.

Devices like the Apple Watch and the Fitbit bands have Food And Drug Administration (FDA) and Common Era (CE) approval for cardiovascular monitoring. Empatica Embrace and BrainSentinel SPEAC are CE marked and have been approved by FDA and EU for detecting convulsive seizures. Empatica Embrace uses accelerometry and EDA to detect the subject's movements and maintains a Bluetooth link to the subject's smartphone, where an application telemeters data and detections to cloud servers and issues caregiver alerts for seizures [18]. BrainSentinel SPEAC is attached by an adhesive patch affixed to the subject's bicep and identifies changes in EMG to detect convulsions. Other CE-marked devices being tested for detecting seizures include Biovotion Everion, ByteFlies Sensor Dots, Livassured NightWatch, Epi-Care Free) [17]. Recent advances in sensing and signal processing technology have resulted in achieving high accuracy in heart rate measurements using wearables devices [19, 20] enabling their use for reliable long-term monitoring.

2.2. Heart rate parameters

The variations in heart rate can be calculated by a number of methods. To classify these, we can calculate them under two main topics as linear and non-linear methods. Linear methods contain time-based and frequency-based methods [15, 21]. Here we list the important parameters considered in this study:

1. Time Domain (Linear)
 - (a) Root mean square of successive differences (RMSSD) [ms]: It is the square root value of the total squared differences of successive NN intervals (time normalized heart beat peaks) with sinus conduction. It is considered as an important indicator of parasympathetic activity [15].
 - (b) Standard deviation of NN intervals (SDNN) [ms]: It is the standard deviation of all normal RR intervals (calculated usually over 24-hours). The standard deviation of NN (SDNN) reflects the parasympathetic component of the autonomic function. SDNN reflects all the cyclic components responsible for variability in the period

of recording [15].

2. Frequency Domain (Linear)

- (a) Low frequency Power (LF Power) [ms^2]: It includes the frequency range between 0.04 Hz and 0.15 Hz and consists of a combination of sympathetic and parasympathetic effects [15, 22].
- (b) High Frequency Power (HF Power) [ms^2]: It includes the frequency range between 0.16 Hz and 0.4 Hz. It is considered to be modulated by the parasympathetic activity of ANS and that is the major determinant of respiratory sinus arrhythmia [15].
- (c) LF/HF Ratio: There is a correlation between LF and HF. The ratio of LF to HF reflects the sympathovagal balance. An increased LF/HF ratio indicates low vagal activation [22].

3. Non-linear methods

- (a) SD1/SD2: SD1/SD2 is a non-linear parameter measure from a Lorenz plot (RR interval vs following RR interval) where SD1 is the standard deviation in the transverse direction and SD2 is that in the longitudinal direction. SD1/SD2 is the ratio between short-term and long-term variation or RR interval or the cardiac sympathetic index [23, 15].

For the part I of the study, we use the HRV parameters RMSSD, LF/HF and SD1/SD2 to compare with temporal changes in function connectivity over short duration. In Part II, we shift our focus to long duration changes with specific focus on parasympathetic activation and so primarily use RMSSD and HF Power in our analysis.

CHAPTER 3

PART I : NETWORK NEUROSCIENCE

3.1. Motivation

In the first part we explore the relationship between temporal changes in the functional network of the brain and changes in the autonomic nervous system measured using heart rate variability parameters.

Previous studies have indicated that seizures have a tendency of activating sympathetic nervous activity, and that parasympathetic activation may be prominent during partial seizures [12, 13, 14]. A clear connection between ANS changes and seizure activity needs to be established. This is challenging, as ANS activity is impacted by external stimuli along with seizure activities, it can vary between seizures in the same individual and it can vary between different individuals [24]. Network theory can be explored to understand such complex relationships.

Recent studies have shown a correlation between HRV and changes in functional connectivity of the brain [25, 26]. The authors built functional connectivity networks using fMRI blood-oxygen-level-dependent imaging (BOLD) and identified regions of the brain that are associated with HRV changes. The regions are part of the central autonomic network (CAN) which are involved with ANS function. We use a similar approach of finding the association between changes in HRV and in functional connectivity using intracranial EEG and ECG signals. Network analysis tools and use of long-term continuous data allows us to have spatial and temporal control of network parameters. This method allows for identification of complex interaction with varying spatial and temporal resolution as compared to traditional time-series analysis. Here, we propose using temporal networks to identify clusters of nodes that associate strongly with time varying changes in HRV. We hypothesize that functional connectivity of specific brain regions is associated more strongly with HRV changes and by extension with ANS activity than other brain regions. Through this we hope to better

understand the links between ANS and brain activity before seizures.

3.2. Methods

3.2.1. Patient Data

The intracranial EEG and ECG dataset used for this study was taken from 12 patients with drug-resistant Temporal Lobe Epilepsy (TLE) admitted at the Hospital of the University of Pennsylvania for pre-surgical assessment. Subjects S1-S6 had left temporal lobe (LTL) seizure onset and subjects S7-S12 had right temporal lobe (RTL) seizure onset. A pre-ictal period from one leading seizure (no seizure activity in the preceding 4 hrs) event was considered for each subject. This was done to minimize influence from previous ictal activity in the data. The demographic details of the subjects have been summarized in Tab. A.1. The de-identified datasets of all subjects were retrieved from the online International Epilepsy Electrophysiology Portal (IEEG.org Portal) [27]. Each of the subjects had a combination of grid, strips and depth electrodes. The number of electrodes considered for each subject for building networks have been listed in Tab. A.1. Along with the EEG recordings, simultaneous Lead II ECG trace was also acquired for each subject. The signals had a sampling rate of 512 Hz (S1-S9) or 500 Hz (S10-S12).

3.2.2. Signal processing

For the analysis, 60-min data from before the start of the seizure was used. First, the EEG data was re-referenced using a common average reference (CAR) montage. Next, the re-referenced data was passed through a 5Hz low-pass Butterworth filter to remove high-frequency noise and only retain low frequency components that capture the slow changes of ANS. This filtered data was then used for community detection. The Brain Connectivity Toolbox (BCT) for Python [28] was used for community detection and network analysis. A 50 Hz low-pass Butterworth filter was applied to the ECG signal to remove high-frequency noise and retain only information about QRS peaks for peak detection. The Biosignal Processing Python library (BioSPPy) [29] and the pyHRV [30] toolbox were used for calculating the HR parameters. The 60-min data was divided into 60 non-overlapping 1-min windows. 1-min

windows were considered to ensure there were sufficient RR peaks in a window for HRV parameter calculations [31].

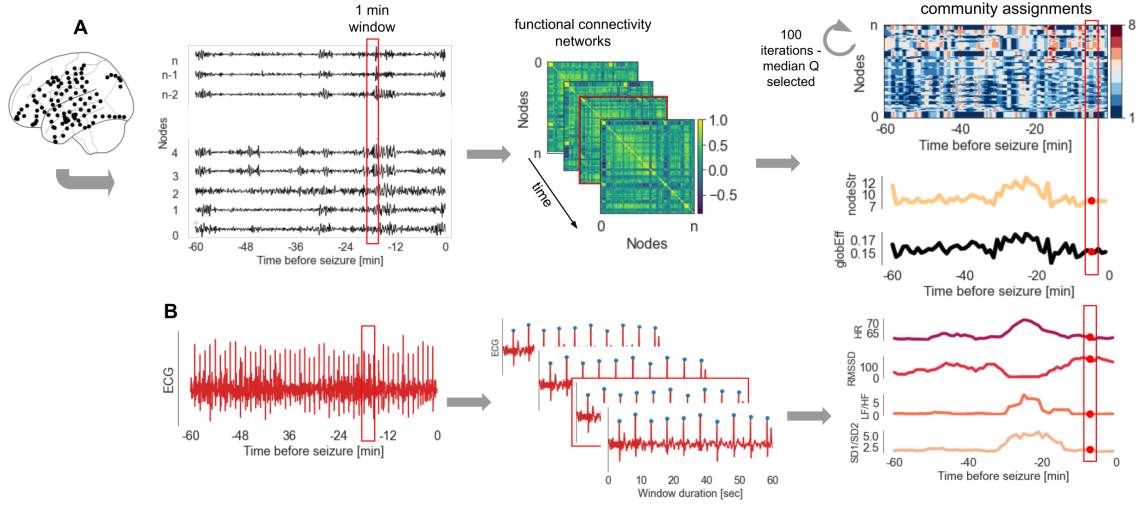


Figure 3.1: Steps in calculation of temporal changes in HRV and network properties

A The processing steps from EEG data to calculation of network properties are shown. EEG data from the intracranial electrodes was divided into 1-min windows. In each window, a functional connectivity network was constructed with electrodes as nodes and Pearson r between electrode pairs as edge weights. The nodes were then assigned communities by optimizing for modularity using the Louvain algorithm. The nodeStr and globEff network properties were calculated for each window.

B The processing steps from ECG signal to calculation of HR parameters are shown. The ECG signal was divided into 1-min windows. In each window, the QRS peaks were detected and the four HR parameters: HR, RMSSD, LF/RMSSD, and SD1/SD2, were calculated from the RR intervals.

3.2.3. Louvain community detection

In each 1-min window, a functional network was constructed using the EEG data. The electrodes formed the nodes and the product-moment correlation coefficient (Pearson's r) as a measure of connectivity between electrode pairs formed the edge weight of the network. The result was a weighted undirected network in each window. The adjacency matrix obtained was thresholded above 0 to only include the positive correlations. The thresholded adjacency matrix was then used for community detection. The Louvain algorithm [32] from the BCT toolbox was used for this. The algorithm identifies optimal community structure by maximizing the number of within-group edge and minimizing the number of between-group edges. In each time-window, the community detection algorithm was run 100 times (with $\gamma = 1$) and the community assignment with the median Q (modularity) was chosen. Considering

the variations in number of nodes (electrodes) across the different subjects, γ of 1 provides optimal size and number of communities (Fig. C.4) [28]. We selected the community with the median modularity as being a good representation of the distribution of modularity values. The selected community assignments in each window were then used for further analysis.

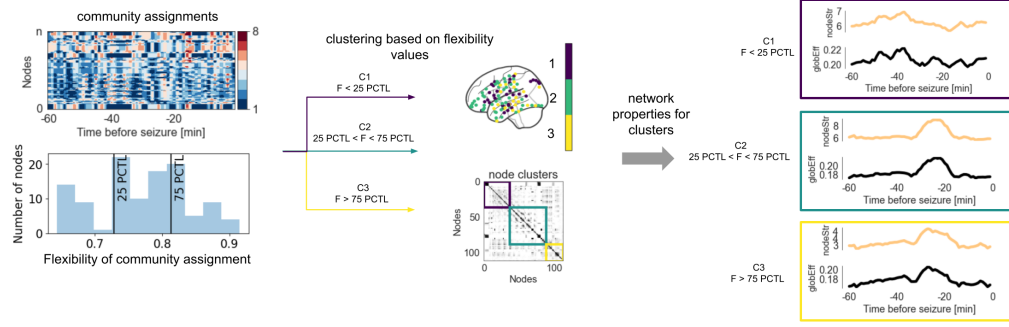


Figure 3.2: Node clustering using flexibility The figure shows the process of dividing the network nodes into three clusters. Flexibility (F) of community assignment of each node was calculated. The nodes with $F < 25$ percentile (PCTL) were grouped as cluster C1, nodes with $25 \text{ PCTL} < F < 75 \text{ PCTL}$ were grouped as cluster C2, and the rest with $F > 75 \text{ PCTL}$ were in cluster C3. For nodes in each cluster, the nodeStr and globEff values were calculated from the adjacency matrix for further analysis with HR parameters.

3.2.4. Node clustering using flexibility

Using the community assignment of nodes across windows, the nodes were divided into three clusters based on the flexibility of each node. Flexibility is a fractional measure that expresses how often a node switches its community assignment over time. It is defined as the number of times a node changes community assignment across time windows normalized by the total number of possible changes [33, 34]. Using the flexibility (F) values, the nodes were divided into three clusters. Three clusters were chosen to denote a low F static cluster, high F dynamic cluster and a middle F moderate cluster. The three clusters were; C1: consisting nodes with $F < 25$ PCTL, C2: consisting nodes with $25 \text{ PCTL} < F < 75 \text{ PCTL}$ and C3: consisting the nodes with $F > 75 \text{ PCTL}$ (Fig. C.2). The cut-off values were chosen to have at least 10 nodes in a cluster to be able to calculate reliable network properties of the cluster.

To quantify the network properties of all nodes and the three clusters, two parameters were calculated. The average node strength of the selected nodes, nodeStr and the global efficiency

of the network, globEff. Node strength has previously been shown to be a good predictor of pre-ictal synchrony [35]. Global efficiency was chosen to represent changes in path length or connectivity over time. The nodeStr and the globEff parameters in each window for all nodes, and the three clusters were smoothed using a 5-window (or 5-min) sliding average across the 60 time windows. These smoothed network parameters were then compared with HRV values.

3.2.5. Heart rate variability parameters

Four parameters were used for this study including HR and 3 HRV parameters: RMSSD, LF/HF ratio, and SD1/SD2. We hoped to get a holistic representation of HRV by considering linear and non-linear parameters with time and frequency domain values. The 1-min low-passed ECG data was processed to detect QRS peaks. These peaks were then used to calculate the four HR parameters using BioSPPy and pyHRV toolbox functions. The resulting HR parameters in each window were smoothed using a 5-window (or 5-min) sliding average across the 60 time windows. These smoothed HRV parameters were then used to correlate with the network parameters.

3.3. Results

We analyzed the relationship between HRV parameters and changes in network parameters of network nodes. We chose two network properties for our comparison, average node strength of all nodes, nodeStr and global efficiency of the network, globEff. These properties were then compared to changes in HRV parameters (Fig. C.1) using Pearson r . To identify clusters of nodes that correlate strongly with HRV parameters, we used node flexibility of community assignments. The network nodes were divided into 3 clusters based on their flexibility values. Fig. C.3 shows the cluster assignments for the different nodes and the r values between the two network properties and each of the four HRV parameters.

After separating the nodes into 3 clusters (Fig. C.2), for the nodes in each cluster, the previously calculated adjacency matrix was used to calculate the network properties, nodeStr and globEff. These values across time windows were then compared to the four HRV

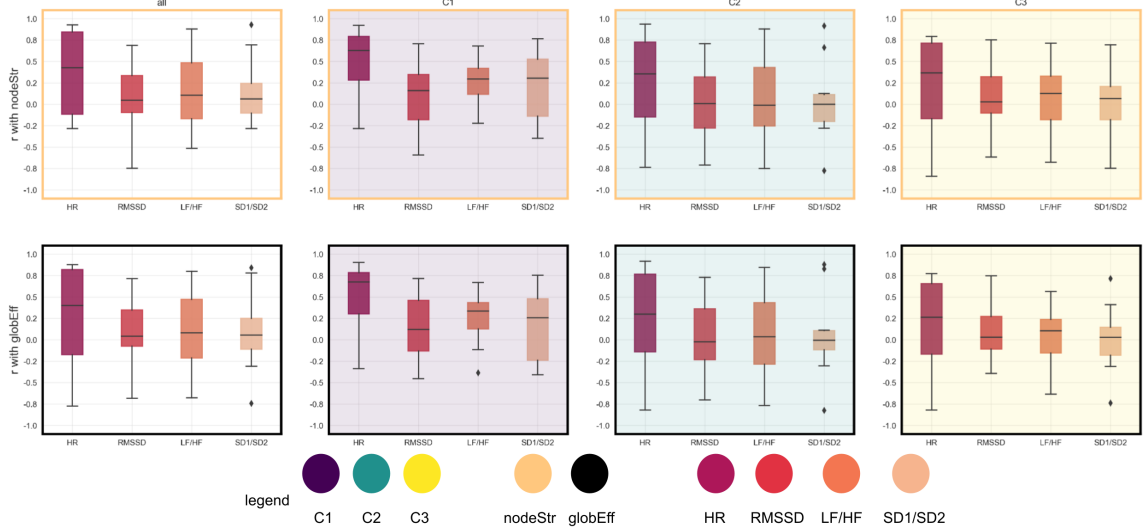


Figure 3.3: Summary of correlation between HRV parameters and network parameters across all subjects The box plots show the distribution of the r values across all subjects. Each box plot shows the distribution of r values between a HRV parameter and network parameter. The top row shows the r values with respect to nodeStr and the bottom row shows the r values with respect to globEff. The first column shows values from all nodes. Columns 2,3, and 4 show values from nodes in clusters C1, C2 and C3 respectively.

parameters using Pearson r . Cluster 1 showed an increased correlation between all the four HRV parameters and both the network parameters as compared to all nodes. The r values of HR and nodeStr were significant ($[-0.28, 0.92]$) for 10 subjects and those with globEff were significant ($[-0.33, 0.90]$) for 11 subjects. Similar trends were seen for the other HRV parameters and network properties of cluster C1. The r trends of cluster C2 and C3 were comparable to that of all nodes combined with HR showing the strongest correlations with nodeStr and globEff. Of the three clusters, cluster C1 nodes indicated stronger association between network properties and all four HRV parameters as compared to all nodes. Of the four HRV parameters, HR has the strongest correlations for each of the three clusters followed by LF/HF ratio. SD1/SD2 had medium to low significant r values for all three clusters. RMSSD had low to non-significant r values with the clusters 2 and 3 and low significant r values with cluster C1. The results showed that the network properties of the nodes with low flexibility associated most strongly with the four HRV parameters and where it was the strongest with HR.

3.4. Discussion

Understanding the relationship between autonomic nervous system (ANS) and pre-ictal brain activity can contribute towards providing behavioral feedback for people with epilepsy. We used four parameters, HR, RMSSD, LF/RF and SD1/SD2 as a measure of ANS. We used temporal networks and node flexibility values to identify a subset of nodes that correlate well to HRV parameters. We found that a small subset of the nodes, about a fourth in number of all nodes, correlate strongly with HRV parameters as compared to all nodes and other subsets. HR had the strongest correlations followed by LF/HF, SD1/SD2 and RMSSD had the weakest correlations to network parameters. This is a step in the direction of understanding the association between pre-ictal brain activity and HRV which can be further used to provide feedback about the behavioral state of people with epilepsy.

3.4.1. Network changes with HRV

Previous research has shown that there are indications of changes in ANS activity before the onset of seizure in terms of ictal tachycardia, ictal bradycardia and changes in low and high frequency components of HR [24, 36, 37, 38]. While these results show promise of establishing the relationship between ANS and pre-ictal brain activity, due to the complex nature of seizure, a definite relationship has not yet been established. Use of network theory can be valuable in understanding such a complex connection between pre-ictal brain activity and ANS. Recent work has demonstrated the connection between fMRI-based functional connectivity (FC) and HRV [25]. The authors built functional networks using fMRI data and found that the connectivity strength between the right thalamus and the ventral attention network increased with an increase in LF power. An opposite trend was observed in healthy subjects. Their work provides indications of changes in behavior of specific brain regions related to HRV expression in patients with epilepsy as compared to healthy controls.

The relationship between HR and FC of brain regions involved in autonomic control was also recently studied [26]. The authors used fMRI scans to build functional networks of specific regions of interest, like the central autonomic network (CAN), which play a role in

ANS function. They were able to establish a direct association between HR and FC in CAN regions, where stronger FC was related to slower HR. This result bolsters the support for using network theory to detect a relationship between HRV parameters and specific brain regions. In a similar work by [39], the authors used fMRI data from which FC was calculated using Fisher z values from correlation coefficients between BOLD values from different brain voxels. They compared FC from two regions of interest (right amygdala and dorsal anterior cingulate cortex) with HRV measurements and found strong positive covariation over a resting state scan for both regions. Most researchers use fMRI to explore the relationship between brain activity and HRV as it provides greater spacial cover as compared to EEG data. Little research has been done to establish a relationship between EEG FC and HRV. Such a dataset has potential for greater temporal resolution and long-term data as compared to fMRI data.

Relationship between HRV and EEG based FC changes has been studied in the context of cognitive flexibility [40]. The researchers used sample entropy of functional connectivity calculated using coherence between electrodes in different frequency bands as a FC measure. They then calculated correlations with HRV parameters similar to our work. They showed that the correlation between HRV and FC is associated with cognitive flexibility. There still remains a lot to understand between changes in brain activity of different regions and corresponding changes in HRV in the context of seizure activity.

In our approach, we used intracranial electrodes with continuous EEG and ECG data from a 60-min pre-ictal window. Using EEG data to build functional networks allowed us to have a continuous 60-min data segment which would not have been easily feasible using fMRI scans. Our network analysis results showed that about a fourth of the nodes in a functional network represent the same or stronger association with HRV parameters as compared to the all nodes of that network. We used node flexibility [34] on community assignments of nodes to group them into 3 clusters. The location of the nodes in the 3 clusters did not have significant spatial segregation across brain regions. Our initial hypothesis was that we would find nodes close to the CAN region to be highly correlated to the HRV parameters

like in [26, 41]. But we found that the cluster C1 which showed the strongest r values with all four HRV parameters had nodes spread across the brain. This could be because of the large clusters we formed consisting of 25% or 50% of the nodes. Identifying clusters with lower numbers of nodes could help to identify focused brain regions that associate strongly with HR. These results show promise of using network theory to identify brain regions that associate with HRV changes in a pre-ictal period.

3.4.2. Limitations and Future work

In our study we considered a limited dataset from 12 TLE patients. A larger study of 20 or more subjects with multiple seizure episodes from each subject will help in identifying more robust associations. We segregated the nodes into three clusters to ensure each cluster has at least 10 nodes for network based analysis. Smaller clusters can be built to identify niche nodes with strong correlation with HRV parameters. Different signal relationship measures like coherence, Fisher z value, network based statistics have shown promise for being sensitive to changes in HRV and need to be explored further. The results show promise of the use of network theory for detection of brain regions that correlate with HRV parameters. The method can further be used in identification of ANS biomarkers for behavioral feedback.

3.5. Conclusion

In this study we used temporal changes in functional networks to identify a subset of nodes that associate strongly with HRV parameters in a pre-ictal period. We divided the network nodes into communities using the Louvain algorithm and then used node flexibility measures to divide the nodes into clusters based on community assignments over time-windows. We found that the node clusters with low flexibility showed strong correlations between network parameters and HRV parameters. We used four parameters, HR, RMSSD, LF/HF and SD1/SD2 values as a measure of HRV. Of them, HR had the strongest correlations followed by LF/HF, SD1/SD2 and RMSSD had the weakest correlations to network parameters. Our study showed how network tools can be used to identify complex temporal relationships between brain activity and HRV before a seizure. We also showed that nodes with low

flexibility in community assignments correlate strongly with HRV parameters. Such a method can be used to identify HRV parameters that correlate strongly with functional brain networks. Establishing such a relationship will help in identifying ANS biomarkers behavioral feedback.

CHAPTER 4

PART II : WEARABLE DEVICES AND BEHAVIORAL STATE DETECTION

4.1. Overview

In this chapter we explore how long duration changes in heart rate variability parameters and wearable devices can be used to detect changes in behavioral states around a seizure. We conducted a clinical trial to record simultaneously, EEG, ECG and event data from the Epilepsy Monitoring Unit (EMU), motion, sleep and heart rate data from wearable devices and ecological moment assessments (EMA) through surveys. We first calculate the agreement between the HR measurements from the wearable devices and the ECG signal. We then analyze the changes in levels of two heart rate parameters: RMSSD and high frequency power to infer behavioral state changes around a seizure.

4.1.1. Funding and Ethics

This study was funded by the NIH Director's Pioneer Award. The ethical approval for the study was provided by the University of Pennsylvania Institutional Review Board (IRB protocol number 849276). The subjects provided informed consent to take part in the study and the permission to use the de-identified data for research.

4.2. Study Design

We recruited patients that were admitted to the Hospital of University of Pennsylvania for pre-surgical assessment of seizures. The patients stayed in the EMU for up to 2 weeks while being connected to scalp or intracranial electrodes for surgical procedure planning, which normally was ablation or resection. We recorded behavior and biometrics during this stay at the EMU. The focus of the study was to identify HR signal parameters and to evaluate the use of commercially available devices for providing feedback about the mood and behavior of the patient. We wanted to record high sampled heart rate data, hand motion data from accelerometer sensors and track sleep patterns.

Table 4.1: Features of selected wearable devices

Fitbit Sense	Apple Watch Series 7
Regularly Logged: 1. Heart rate (a) 0.2 Hz normally (b) up to 1 Hz during activity 2. Sleep tracking	Regularly Logged: 1. Heart rate (a) <0.1 Hz normally (b) up to 1 Hz during activity 2. Sleep tracking 3. Accelerometer (Using SensorLog[42] App) at 50 Hz 4. Respiration rate 5. SDNN
Other features logged intermittently: 1. Activity tracking 2. skin temperature during sleep 3. Respiration rate during sleep 4. Oxygen saturation during sleep 5. Electrodermal activity when triggered 6. 30s ECG recording when triggered	Other features logged intermittently: 1. Activity tracking 2. Skin temperature during sleep 3. 30s ECG recording when triggered

After a careful comparison with options available in the market, we chose 2 wearable devices for our study, the Fitbit Sense (Alphabet, Inc., released 2020) and the Apple Watch Series 7 (Apple, Inc, released 2021). A list of features of these devices is provided in Tab. 4.1

4.3. Trial Data Collection

Once the subject was admitted to the EMU, they were given one of the two watches to wear for the duration of their stay. We charged the watch once/twice a day depending on the battery drain. For some subjects, we switched on activity tracking to log heart rate at a higher (up to 1Hz) sampling rate. The watch was synced with a study phone (Apple iPhone, Apple Inc.) during charging to save all the measured data on the phone. The Fitbit Sense was synced with the Fitbit iOS app. The data from the Apple Watch was synced with the Apple Health App. Additionally for the Apple Watch, we used the SensorLog app [42] to continuously log 3-axis accelerometer data at 50 Hz which was not possible from the default

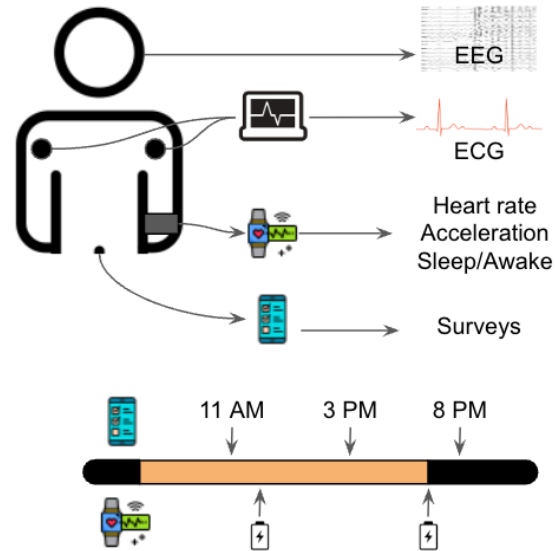


Figure 4.1: Clinical Trial data streams

Table 4.2: Data streams from clinical trial

Clinical data	Wearables	Surveys
<ol style="list-style-type: none"> 1. Intracranial/scalp EEG 2. Lead II ECG signal 3. Clinical annotations : seizures, activity, other clinical observations 4. Medication data 	<ol style="list-style-type: none"> 1. Heart rate 2. Sleep stages 3. Movement 	<ol style="list-style-type: none"> 1. 3 timed surveys of 5 questions 2. Free form survey responses

Apple Health app. The data streams from the trial are illustrated in Fig. 4.1.

The data collected from the wearables was saved in a secured cloud server managed by Center for Neuroengineering and Technology (CNT). The EEG, ECG signals and annotations from the hospital were saved on IEEG.org Portal [27].

4.4. Signal Processing

Signal processing and analysis of the data was performed using Python 3.

4.4.1. Fitbit Sense

Data exported from the Fitbit sense was available as *.json* files which were parsed to obtain timestamped heart rate data at up to 1Hz sampling. The sleep stage data was available as start and stop times of sleep each day and during that time, further details of stages such as *wake, light, rem, deep* were provided.

4.4.2. Apple Watch

Data exported from the Apple Health app was processed with the help of open source Python tool, Quantified self [43]. The time stamped heart rate signal was available at a sampling rate of up to 1 Hz. Sleep stage data indicating whether the subject was asleep or awake was also available from the watch.

The Apple watch does not provide a long-term background accelerometer data logging feature as part of their Apple Health app, but an Application Program Interface (API) to record accelerometer data is available. We used the SensorLog app [42], which uses this API, to record accelerometer data at 50 Hz. The app provided time stamped data of 3-axis accelerometer values as *.csv* files.

4.4.3. ECG

ECG data was available for each subject from IEEG.org. The sampling rate of the signal was 1024 Hz for intracranial subjects and 256 Hz for scalp subjects. To process the ECG signal, the BioSPPy [29] and the pyHRV [30] toolbox were used for calculating the HRV parameters. First the raw signal was passed through a 0.05 Hz notch filter to remove baseline

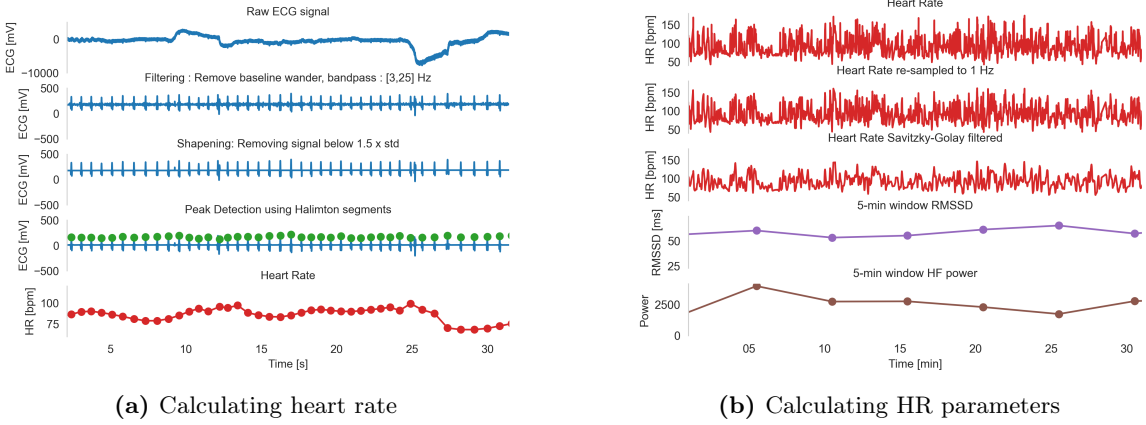


Figure 4.2: ECG signal processing

wander. Then it was passed through a band-pass filter of [3,25] Hz to remove high frequency noise and low frequency wanders. The QRS peak was then sharpened by dividing the signal into 5s segments and by equating the signal below 1.5x standard deviation to the mean of the 5s window. This was a novel approach that helped reduce the number of stray spikes that were not filtered. Then using the BioSPPY toolbox with Hamilton segments, peaks were identified and heart rate was calculated. The heart rate signal was re-sampled to 1Hz. At this point, if the dataset had 2 ECG channels, the minimum of the 2 HR values for each second was considered. HR signal was then passed through a 3rd order Savitzky-Golay filter of 11 sample windows (or approx. 10s). This smoothed the noise of the signal while retaining the variability.

Two HRV parameters, RMSSD and HF power were calculated in non-overlapping 5-min windows from the heart rate obtained from the watch and ECG.

4.5. Results

4.5.1. Summary of HR data collected

In total, 7 subjects were recruited for the trial, 2 with scalp EEG and 5 with intracranial EEG. We used the Fitbit Sense for the first two subjects due to its high data sampling and long battery life. We then switched to Apple Watch for the remaining subjects to log accelerometer data. Fig. 4.3 provides an overview of the HR data collected from the

Table 4.3: Patients summary

Subject ID	Age	Sex	EEG type	Device	Acc Data
LB3_001_phaseII	23	M	intracranial	Fitbit Sense	No
LB3_002_phaseI	20	F	scalp	Fitbit Sense	No
LB3_004_phaseI	40	M	scalp	Apple Watch	Yes
LB3_004_phaseII	32	F	intracranial	Apple Watch	Yes
LB3_005_phaseII	40	M	intracranial	Apple Watch	Yes
LB3_006_phaseII	51	F	intracranial	Apple Watch	Yes
LB3_007_phaseII	36	F	intracranial	Apple Watch	Yes

watches and ECG signal and the corresponding HRV parameters calculated. The gray shaded regions indicate when the subject was asleep as detected by the watch. The dotted vertical lines indicate (for LB3_001_phaseII, LB3_004_phaseI and LB3_005_phaseII) seizures annotated by the clinical staff. Seizure annotations from the remaining subjects needed further verification. The gaps in the blue traces from the wearables indicated that the device was removed for charging, its battery died prematurely or the trial was paused for logistical or clinical reasons (LB3_002_phaseI and LB3_005_phaseII). Data from LB3_004_phaseII was discarded due to complications in processing of clinical data.

4.5.2. HR sampling and delay between ECG and watch

Next, we compared the agreement between the HR and HRV values calculated from the ECG signal and the watch. First we computed the time lag between the 2 signals. For this we considered a 6-hour segment on day 2 after the watch was put on the subject. We calculated a 5-min average of the HR value to account for difference in sampling between the 2 signals. We used cross-correlation between the 2 signals to compute the delay. HR data from all subjects except LB3_002_phaseI had negligible lag between the 2 signals. Data from LB3_002_phaseI had fluctuating lag for different segments [-20s, 190s]. Digging deeper indicated that changes in lag were due to a noisy signal and changes in sync after the watch was charged. When RMSSD and HF were compared, the lag was negligible or absent in different segments and so no action was taken and the signals were used as is.

The heart rate from the ECG signal was manually re-sampled to 1Hz to match the maximum

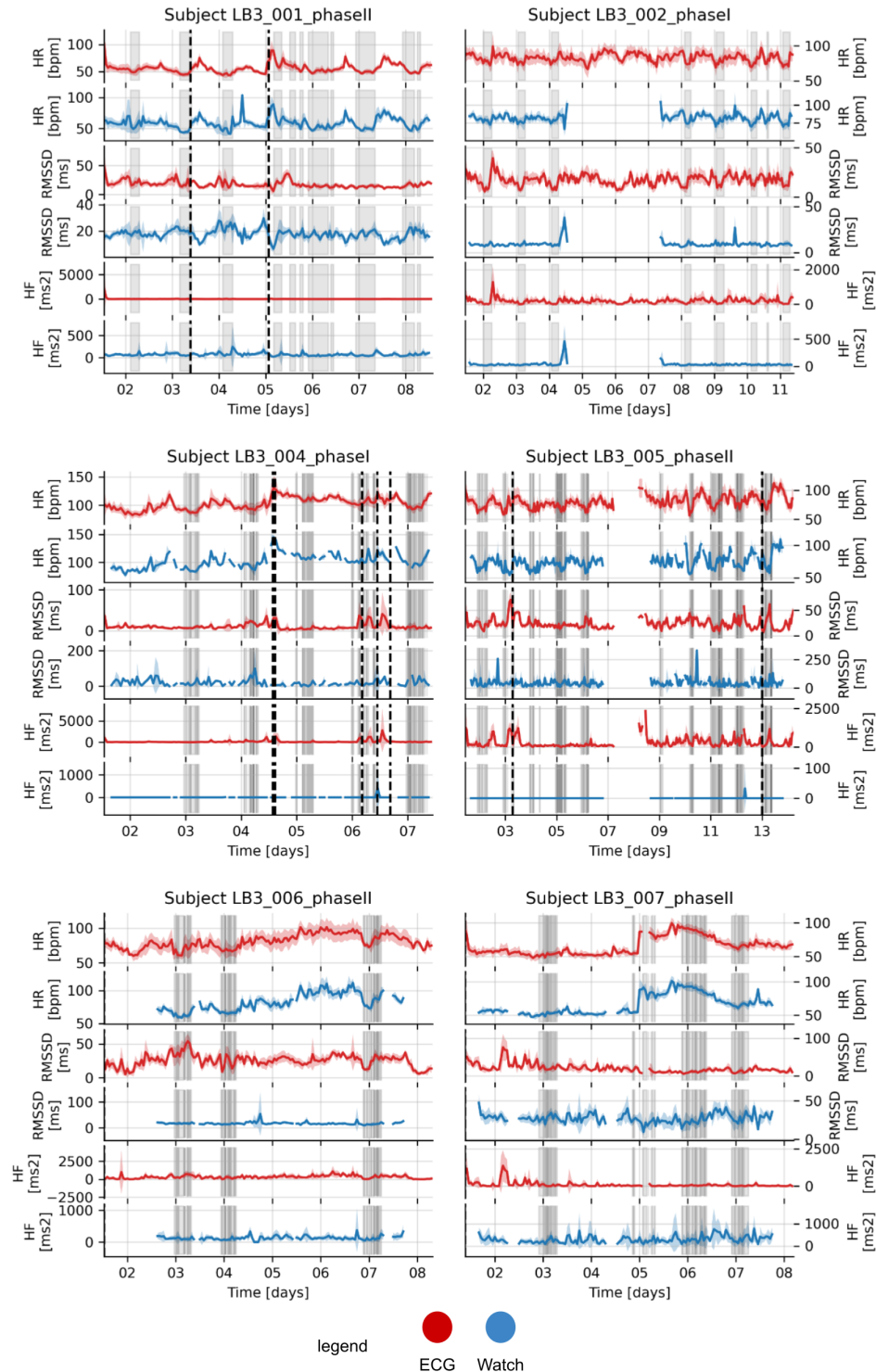


Figure 4.3: Overview of HR data collected HRV parameters calculated for all subjects The plots show the heart rate, RMSSD and HF power data from ECG and study watch collected. The gray shaded regions indicate when the subject is asleep as detected by the watch. The dotted vertical lines indicate seizures annotated by the clinical staff. The gaps in the data indicate data loss or pause of the trial for clinical reasons.

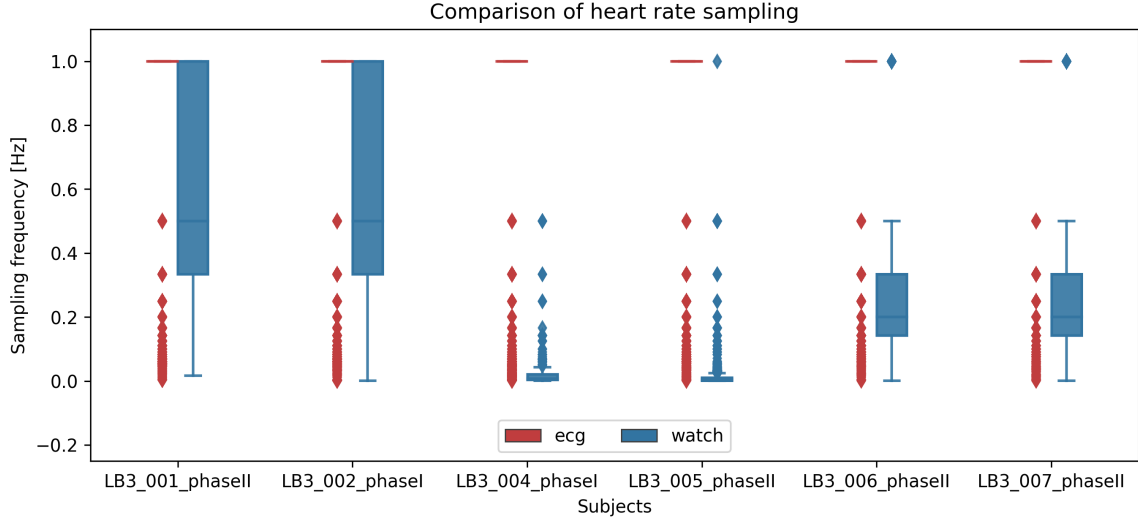


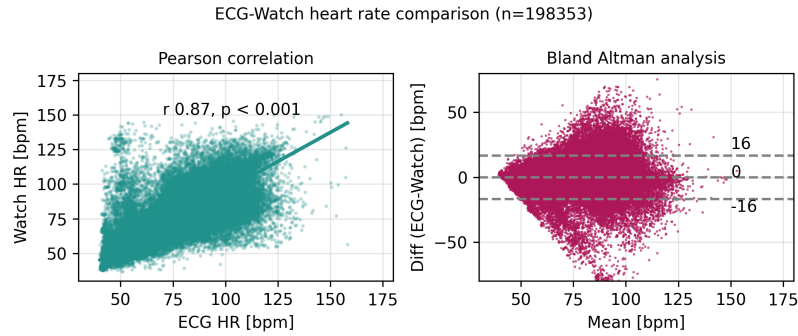
Figure 4.4: Comparison of heart rate sampling The plot shows the distribution of sampling intervals between HR measurements recorded for different subjects. For ECG the data was manually re-sampled to 1Hz

sampling of the watches. In Fig. 4.4 we can see the varying sampling of recorded HR values between different subjects. The Fitbit Sense was used for LB3_001_phaseII and LB3_002_phaseI. We switched on workout/activity tracking on the watch to record heart rate at a high sampling rate. Without activity tracking, the Fitbit logged heart rate 0.2 Hz (once in 5s). With the workout tracking switched on, we got a sampling rate of up to 1 Hz with a mean sampling rate of 0.5 Hz.

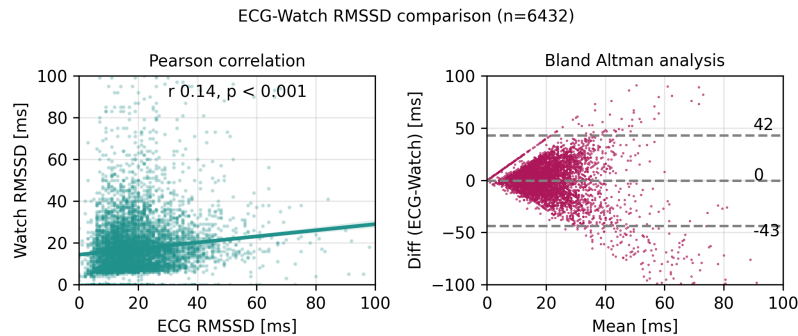
Apple watch had a mean sampling rate for $\text{HR} < 0.1 \text{ Hz}$. Increasing the sampling rate by switching on workout mode, drastically impacted its battery life. For subjects LB3_004_phaseI and LB3_005_phaseII we kept the activity tracking off to allow the watch to record data for 20-23 hours on one charge cycle. For subjects LB3_006_phaseII and LB3_007_phaseII, we switched on the workout tracking and charged the watch 2 times a day. We saw an increase in average sampling rate to 0.2 Hz for these subjects.

4.5.3. Agreement between HR and HRV from watch and ECG

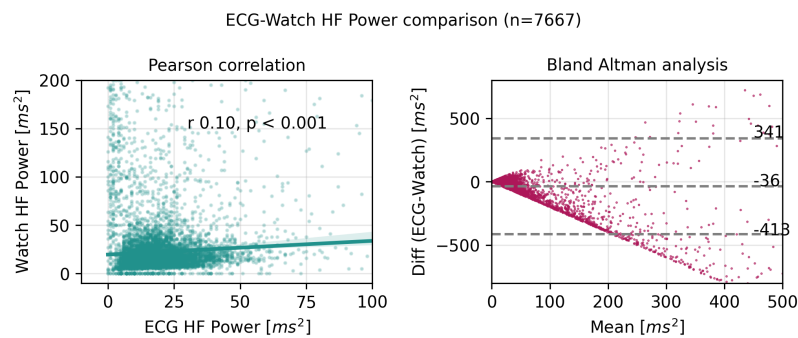
Next, we checked how well the HR and HRV measurements from the ECG and watch agreed with each other. We used Pearson correlations and Bland Altman's limits of agreement [44]



(a) Heart rate



(b) RMSSD



(c) High frequency power

Figure 4.5: ECG vs Watch comparing HR and HRV values for all subjects. The Pearson correlation plot shows the regression line that fits the data the best. The Bland Altman plot shows the dashed line for mean, and 2 lines showing the limits of agreement for a confidence interval of 95% coverage of the difference between the 2 measurements.

analysis. The Bland Altman method is commonly used to compare measurements from 2 different devices and has been used to validate Apple Watch measurements [20]. Using this method, we calculated the mean difference between two methods of measurement (the ‘bias’), and 95% limits of agreement of the mean difference ($1.96 \times$ standard deviation on both sides of the mean difference). It is expected that the 95% limits include 95% of differences between the two measurement methods. The presentation of the 95% limits of agreement is for visual judgment of how well two methods of measurement agree. The smaller the range between these two limits the better the agreement is between the two measurements [45].

For comparing HR, the HR values were re-sampled to mean values in 1s windows and only those timestamps when there was a value from the watch and ECG was considered. For comparing the HRV values of RMSSD and HF power, the HRV values were calculated in 5-min windows and only samples at timestamps when there was a HRV value from the watch and ECG was considered.

In the summary plot from all subjects Fig. 4.5, we see a good agreement ($r=0.87$) in the HR values, with the limits of agreement at [-16, 16] for 95% coverage of the difference between the 2 signals. When we refer to the plots of individual subjects in Fig. 4.6, we see that subjects with Apple watch had higher correlation values as compared to ones with Fitbit, with the highest correlation of $r=0.96$ for LB3_007_phaseII. For the subjects where data was recorded from the Fitbit, the highest correlation was $r=0.69$ and they also had wider limits of agreement indicating lower agreement.

Looking at the HRV parameters in Fig. 4.5, we see that the overall $r=0.14$ for RMSSD and $r=0.1$ for HF power, indicating poor correlation between the two. The limits of agreement for RMSSD and HF power were also high at [-43, 42] ms for RMSSD and [-413, 341] for HF power. When we look into individual subjects, we see that for most cases, large variation is seen along the ECG axis (x) and smaller variation is seen for the watch axis (y). This could be due to the sparse sampling of the HR data resulting in lower HR variability being captured as compared to HR from ECG. This was also supported by the observation that

LB3_001_phaseII, LB3_002_phaseI and LB3_007_phaseII have the highest correlation values for RMSSD and they also had the highest sampling rates.

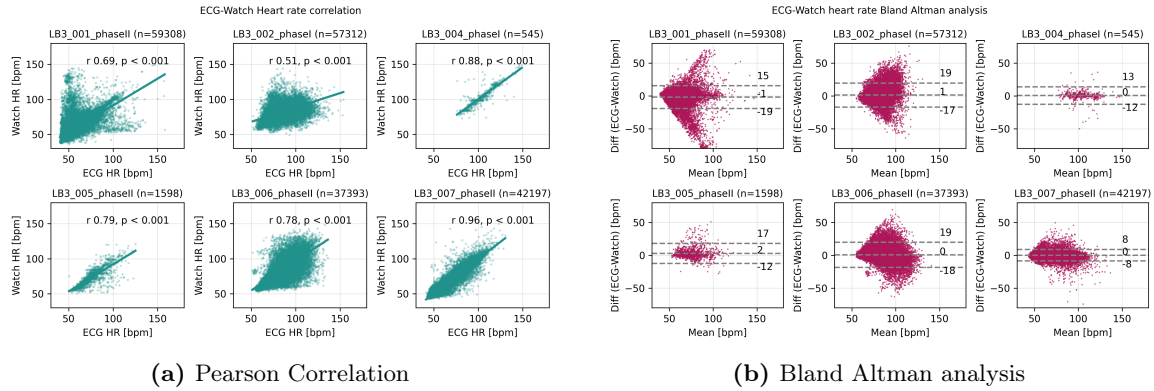


Figure 4.6: ECG vs Watch comparing individual Subjects : Heart Rate

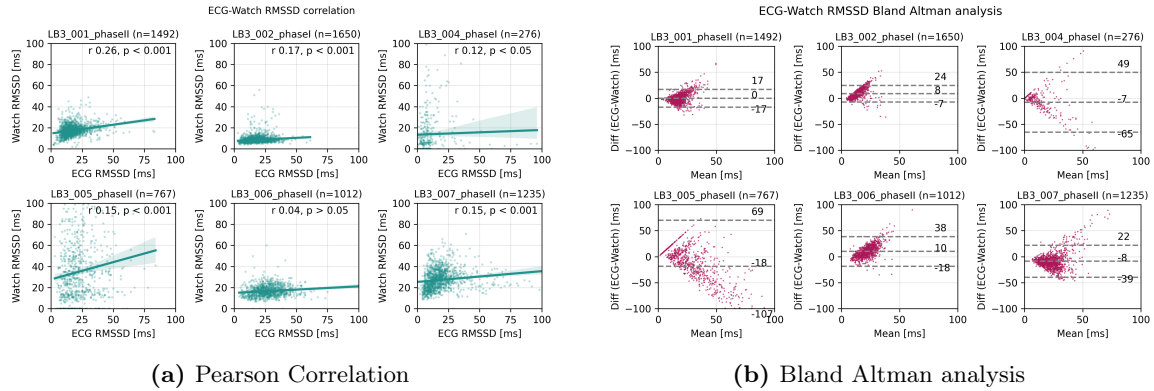


Figure 4.7: ECG vs Watch comparing individual Subjects : RMSSD

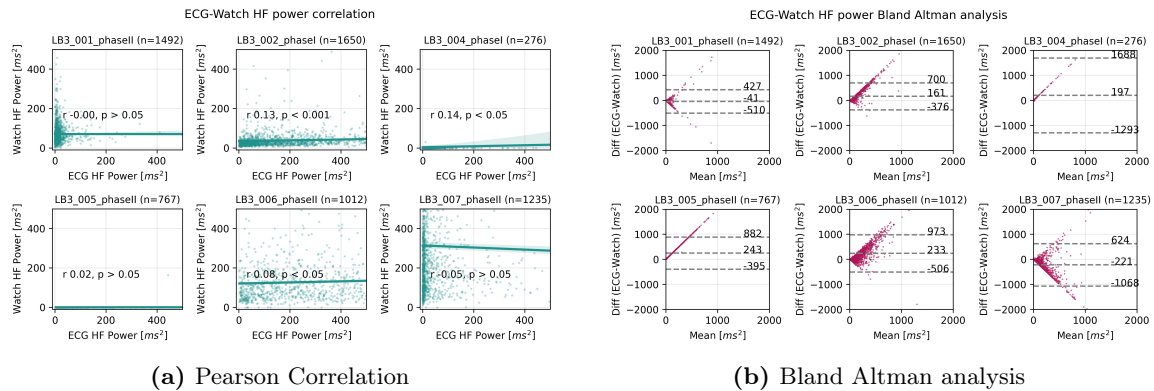


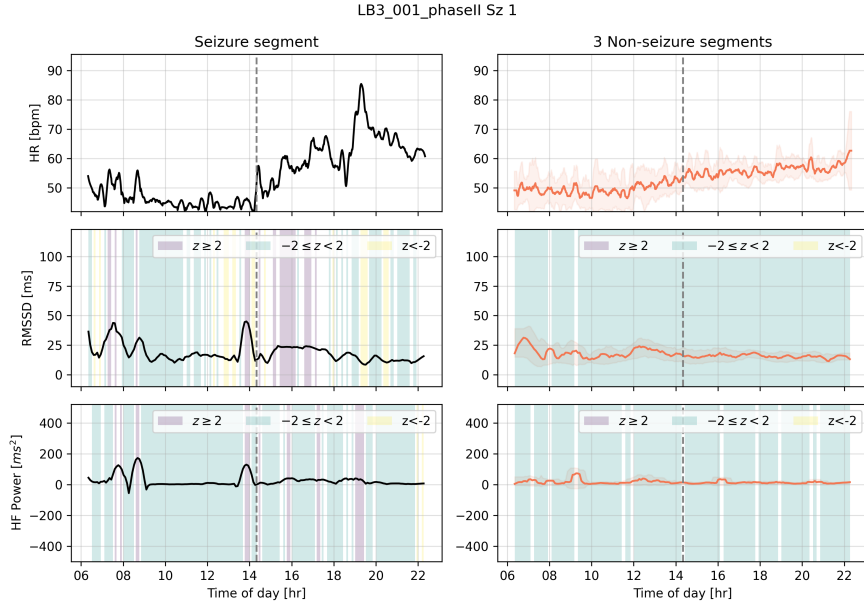
Figure 4.8: ECG vs Watch comparing individual Subjects : High frequency power

4.5.4. HRV states around seizure

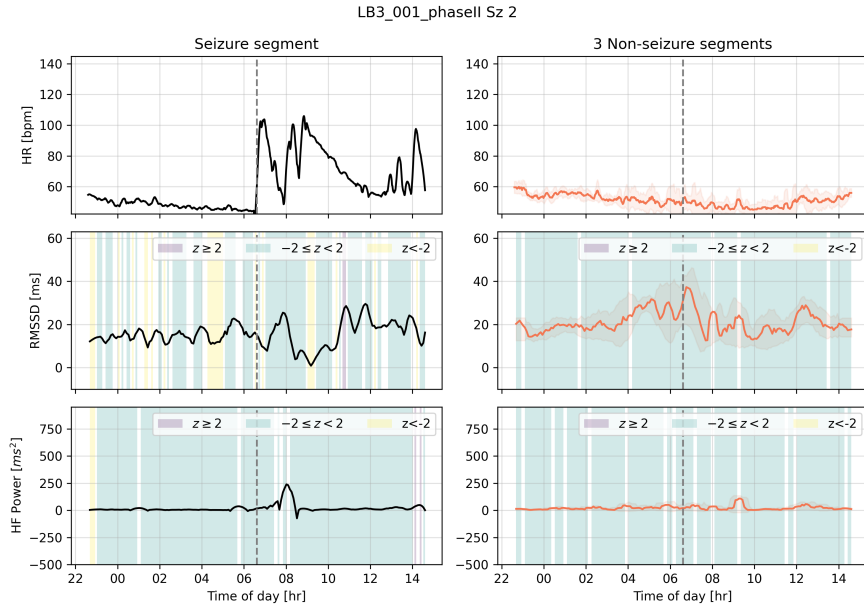
After comparing the watch measurements and the ECG measurements, we next analyzed the changes in HR and HRV before and after a seizure. We hypothesized that behavioral changes and indications of stress before seizure would be captured by the changes in RMSSD and HF power. To analyze this, we considered data from 8 hours before and 8 hours after a seizure. If there were a cluster of seizures, we choose 8 hours before the first seizure and 8 hours after the last seizure in the cluster. We then compared the changes in parameters around the seizure to a baseline of non-seizure days. Due to the low agreement between the HR values from ECG and the watch data, we chose to use the HRV values calculated from the ECG signal for this analysis.

To calculate baselines values, for every seizure, we considered data for the same time-window (± 8 hours around seizure time) on 3 non-seizure days during the stay at the EMU. These days were before and after the selected seizure depending on when the seizure occurred and duration of stay. We then calculated hourly mean and standard deviation values of RMSSD and HF power from these 3 non-seizure time segments. We then calculated HRV states around a seizure. We took the HRV values at a given time instant and calculated the z-score by subtracting the mean and standard deviation of that hour from the baseline values. The values from the corresponding hour were taken to account for fluctuations due to circadian rhythm throughout the day. These z-score values were used to divide the segment into 3 states, Low ($z < -2$), Medium($-2 \leq z < 2$) and High($z \geq 2$) z-values. This can be seen in Fig. 4.9, Fig. 4.10 and Fig. 4.11.

For LB3_001_phaseII (Fig. 4.9) Sz 1 there is a period of high state of RMSSD and HF power an hour before the seizure which dropped right before the start of the seizure. In Sz 2 we do not observe such a pattern and the HRV values for the seizure and non-seizure segments were not statistically different. We however saw that for Sz 2 the HR values had a sharp increase after the seizure and the value dropped over a 4-hour window after the event.

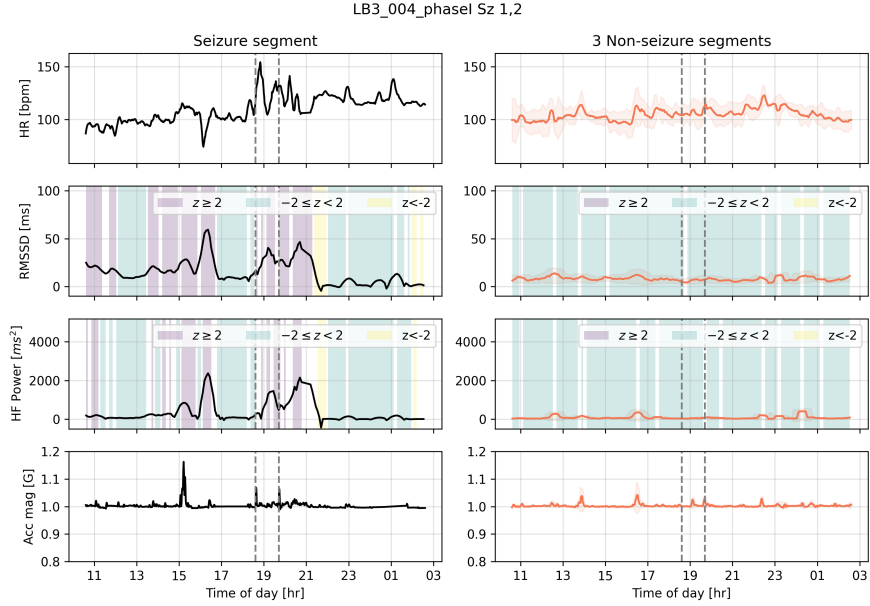


(a) Sz 1

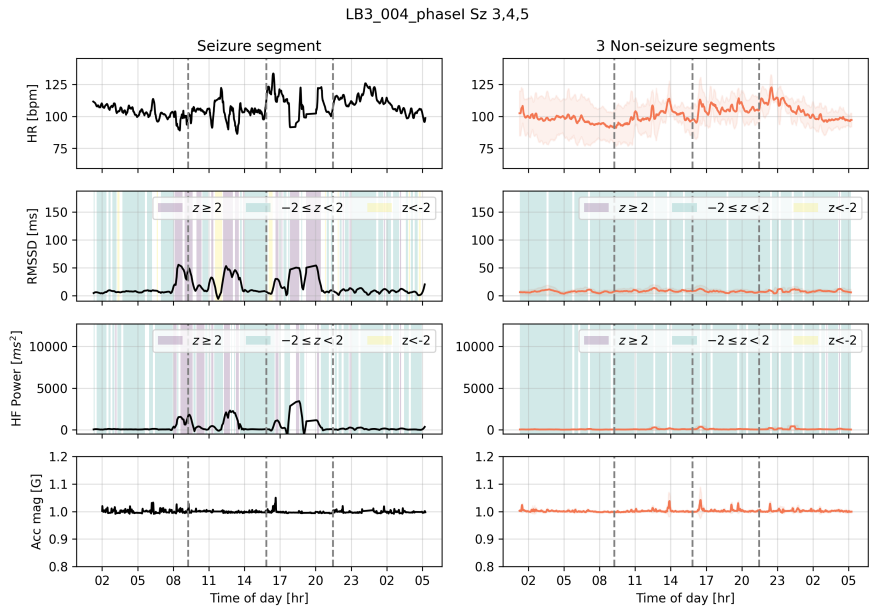


(b) Sz 2

Figure 4.9: HRV stages : LB3_001_phaseII. The plots show the data from a seizure segment and corresponding data from 3 non-seizure days. The dotted line indicates the seizure which lasts up to a few minutes. The RMSSD and HF power plots indicate HRV states. The HRV values were compared to hourly baselines from non-seizure days to compute z-scores. The 3 states correspond to Low ($z < -2$), Medium($-2 \leq z < 2$) and High($z \geq 2$) z values.



(a) Sz 1,2



(b) Sz 3,4,5

Figure 4.10: HRV stages : LB3_004_phasel The plots shows the data from a seizure segment and corresponding data from 3 non-seizure days. The dotted line indicates the seizure which lasts up to a few minutes. The RMSSD and HF power plots indicate HRV states. The HRV values are compared to hourly baselines from non-seizure days to compute z-scores. The 3 states correspond to low ($z < -2$), medium($-2 \leq z < 2$) and high($z \geq 2$) z values.

For LB3_004_phaseI in Fig. 4.10a we see 2 seizures about 1 hour apart and in Fig. 4.10b we see 3 seizures about 6 hours apart. Looking at the HRV states, Sz 1 and Sz 4 had a similar pattern of Medium state before a seizure and period of High states after. Across seizures we did not observe a common trend of state before or after a seizure. We also acquired accelerometer data for this subject. We calculated the magnitude value from the 3 X,Y and Z values. No statistical difference is observed leading up to a seizure as compared to a non-seizure day.

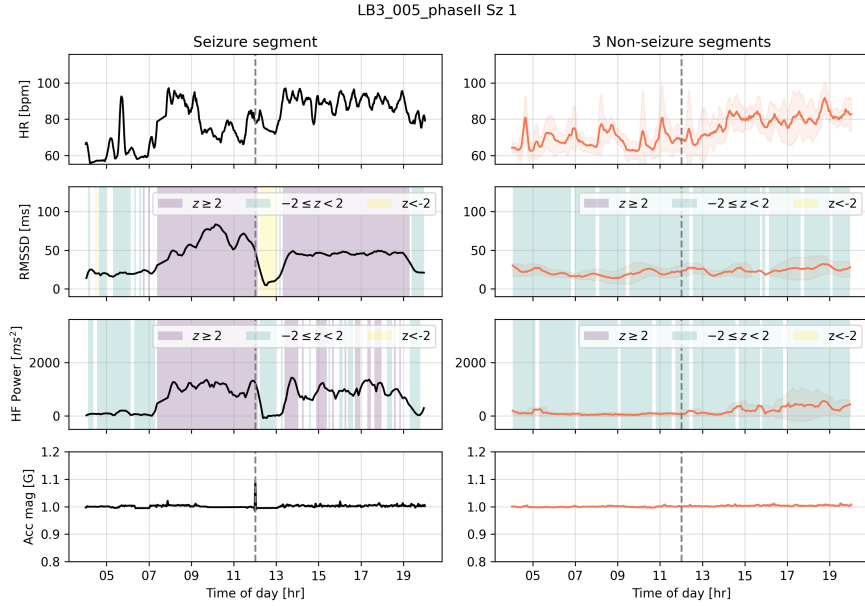
For LB3_005_phaseII in Fig. 4.11a we observed a state from High before a seizure that started 4-hours prior a seizure and it transitioned to Low state for RMSSD and Medium state for HF power after the seizure. For Sz 2 in Fig. 4.11b we saw a rise to High state about 1.5 hours before the seizure which gradually shifted down to Low state closer to the seizure. After the seizure, both RMSSD and HF state gradually rose to High in about 8 hours.

4.6. Discussion

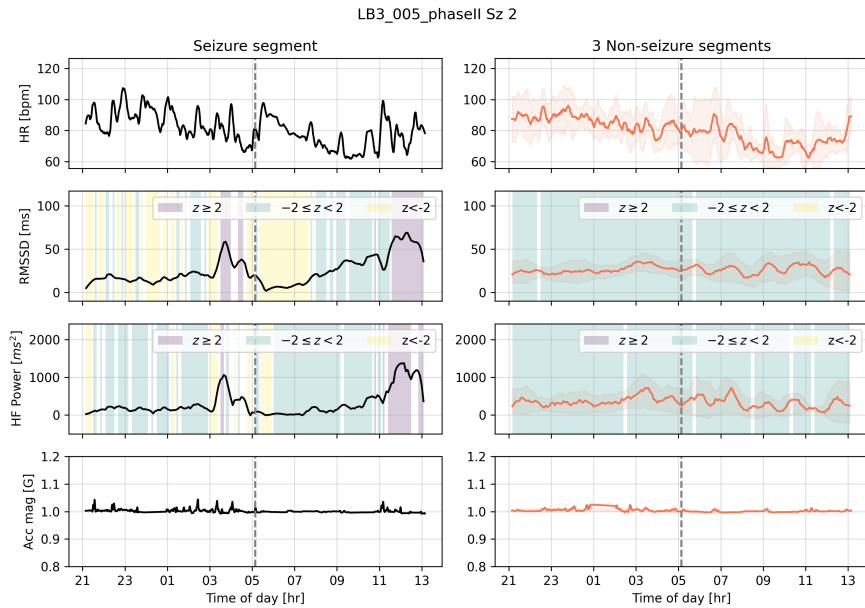
In this part of the study we aimed to evaluate the use of wearables to measure biometric signals from people with epilepsy and to identify behavioral state changes around a seizure. We recorded heart rate, sleep/awake state and motion data from 7 patients who were in the EMU for pre-clinical assessment. We used 2 devices, a Fitbit Sense and an Apple Watch Series 7 for our analysis.

4.6.1. Challenges with wearable devices

For collecting data from the wearable devices, the Fitbit Sense had a battery life of up to 2 days with activity tracking on and up to a week with tracking off. We synced it with the Fitbit app once a day. In contrast, the Apple watch had a battery life of up to 1 day with activity tracking on and up to 20 hours with tracking on. This resulted in the need to charge the watch up to 2 times a day for 60-90 mins. We lose data during these segments and add to the logistical load of conducting the trial. Currently, there is no direct way of recording or logging raw accelerometer data from the Fitbit watch. To record accelerometer values, the Apple watch or other devices like the Embrace (Empatica, Inc.), EpiCare@Home



(a) Sz 1



(b) Sz 2

Figure 4.11: HRV stages : LB3_005_phaseII The plots show the data from a seizure segment and corresponding data from 3 non-seizure days. The dotted line indicates the seizure which lasts up to a few minutes. The RMSSD and HF power plots indicate HRV states. The HRV values are compared to hourly baselines from non-seizure days to compute z-scores. The 3 states correspond to Low ($z < -2$), Medium($-2 \leq z < 2$) and High($z \geq 2$) z-values.

(Byteflies, Inc) can be used. To solve the problem of the data loss from the Apple watch during charging, 2 Apple watches can be used and "hot-swapped" when one is discharged. Apple Health app allows for 2 watches to be used and can switch between them to ensure it is synced to the correct device.

Repeated removal of the device and switching it on-off can also impact the data sync. We observed measurable delay of HR signal only for one subject that used the Fitbit watch. No such delays were observed for the data from the Apple watch.

Comparing the HR data, the Apple watch showed higher agreement with the HR from ECG as compared to Fitbit. The Fitbit Sense had a higher average sampling of HR values but lower agreement with HR from ECG. When comparing the RMSSD and HF values, we saw a very low agreement between the wearable devices and the values from ECG. This could directly be attributed to the lower sampling of the HR values from the watches resulting in lower variability. As a future step, it would be favorable to record and process higher sampled HR data on the watch to calculate variability measures.

4.6.2. Behavioral state detection

We aimed to use HRV parameters to identify behavioral states around a seizure. We used hourly average values from 3 non-seizure days to form the baseline measurements for RMSSD and HF power. Around a seizure, we compared the RMSSD and HF values to baseline to identify Low, Medium and High states. Both RMSSD and HF power have been observed to be associated with the parasympathetic activity of the ANS [15, 46] RMSSD has also been used as a biomarker for Sudden Death on Epilepsy (SUDEP) [47] risk, where the authors showed that lower RMSSD values were associated with higher risk of SUDEP.

Here, we used z-scores of RMSSD and HF values to identify time duration of High, Medium and Low states. In the sample of 9 seizures from 3 subjects, we saw that the RMSSD state decreased from a higher state to a lower states before a seizure starts. Such a drop in RMSSD has also been observed in athletes after a training activity [48]. The authors showed that

RMSSD drops after high training load. This is possible indication of fatigue. We observed a High/Medium state in RMSSD, upto 2 hours before the seizure, followed by a drop in state for most seizures. This could be an indication of fatigue as we get closer to the seizure and the rise in state a few hours after the episode could be an indication of recovery from the seizure. Similar observations have been made in short 2-min windows of HRV values like LF/HF around a seizure in newly diagnosed TLE patients [49]. We will have to expand our analysis to a larger set of patients and seizures to validate this observation. We will also explore the use of multiple biometric measures such as HRV parameters and movement data from accelerometry to identify behavioral pattern changes before and after a seizure.

We used non-seizure days before and after a seizure to establish a baseline, future methods could use longer duration segments distant from a seizure occurrence as a non-seizure day in the EMU may not truly represent the baseline of the subject. This is an area where the use of wearable devices would be vital for long-term monitoring of biometrics.

4.7. Conclusion

We showed the accuracy of HR measurements using the Fitbit Sense and Apple Watch in an EMU setting. We identified the strengths and weaknesses of the devices and offered suggestions to improve data collection and signal quality. We also explored a method to identify behavioral states around a seizure using HRV values. The method presented shows the potential of identifying behavioral state changes in people with epilepsy, with indications of stress and fatigue before the start of a seizure. To validate the observations, a larger dataset of seizures and patients will be required.

CHAPTER 5

CONCLUSION

During my thesis, I worked under Dr. Brian Litt at the Center of Neuroengineering and Technology at the University of Pennsylvania where I was able to combine my interest in exploring the use of biometric signals from wearable devices for seizure management. With my past experience in biomedical sensing and heart rate measurements, I was interested in identifying the connection between behavioral changes, changes in heart rate and brain activity around a seizure. Through this thesis I took the first step in exploring this relationship. We had two main objectives. One, to evaluate the use of wearable devices to measure biometric signals like heart rate, motion and two, to find an association between different biometric signals and brain activity. With this the hope was to identify the shortcomings of biometrics measured from wearable devices and plan the next steps to use these devices for behavioral feedback for people with epilepsy. At the start of my thesis we designed a clinical trial to simultaneously record data in the EMU and through wearable devices. This would provide high resolution EEG data, which forms the gold standard for seizure activity along with biometrics from wearable devices which has the potential for continuous long term monitoring. As we prepared for this trial, we had past data of subjects from the EMU with EEG data and ECG data. We used temporal changes in functional networks to identify a subset of nodes that associate strongly with HRV parameters in a pre-ictal period. We found HR to associate strongly with this global network parameter. This method showed the potential of finding the complex relationship between brain connectivity and behavioral changes using HR values. As a next step we will dig a little deeper into this area to explore temporal connectivity changes in specific brain regions in the temporal lobe that are known to be associated with stress and ANS activity.

Behavioral changes tend to have longer time scales so using wearable devices that can record data over weeks and months becomes important. A bulk of my time over the past few months was spent collecting data from the trial and developing the processing pipeline to prepare the

data for analysis. We recruited 7 subjects with an average stay of 10 days in the EMU. This formed the pilot study to evaluate the use of wearable devices for measuring HR, motion and sleep. From the data collected, we observed that the Fitbit Sense recorded HR at a higher sampling rate as compared to Apple Watch. But Apple watch HR measurements had higher accuracy and agreement with ECG based HR. The Fitbit Sense had a multi-day battery life allowing for ease of data collection while the Apple watch needed to be charged twice a day at times. Due to the sparse sampling of HR, HRV values of RMSSD and HF power had low agreement with ECG based measurements. Further analysis of the disagreement with a larger sample size is required. We also tried using hourly average values of RMSSD and HF values on non-seizure days as a baseline to calculate z-score values around time of a seizure to identify behavioral states of Low, Medium and High z-scores. From the 9 seizures of 3 subjects, we saw that the RMSSD state decreased from a higher state to a lower states before a seizure starts. Similar observations have been made in athletes after a training activity and could be an indications of stress or fatigue before the start of a seizure. We will have to expand our analysis to a larger set of patients and seizures to validate this observation.

In summary we have contributed the following:

1. Demonstrated the use of network neuroscience to find an association between temporal changes in functional connectivity of the brain and changes in heart rate before a seizure.
2. Evaluated two commercially available wearable devices for continuous monitoring of HR and their use for people with epilepsy. We identified the strengths and weaknesses of the devices and offered suggestions to improve data collection and signal quality.
3. Presented a method to compute behavioral state changes before and after a seizure using heart rate variability parameters.

APPENDIX A

SUBJECT DETAILS

Table A.1: Patient details for Part I : Network Analysis

Sub. Num.	Sub ID	Sex	Age Surg.	Age Onset	Loc.	Sz. Dur. [s]	Num. elec.	Slp/Awk
S1	HUP74_phaseII	F	25	5	LTL	76	114	Sl
S2	HUP75_phaseII	F	55	52	LTL	673	112	Sl
S3	HUP78_phaseII	M	54	0	LTL	36	101	Aw
S4	HUP86_phaseII	F	25	NA	LTL	79	110	Aw
S5	HUP80_phaseII	F	41	NA	LTL	63	100	Aw
S6	HUP88_phaseII	F	34	1	LTL	218	53	Aw
S7	HUP65_phaseII	M	36	2	RTL	79	64	Sl
S8	HUP68_phaseII	F	26	15	RTL	107	86	Sl
S9	HUP82_phaseII	F	56	34	RTL	637	86	Aw
S10	HUP094_phaseII	F	48	20	RTL	59	83	Sl
S11	HUP105_phaseII	M	39	27	RTL	50	55	NA
S12	HUP107_phaseII	M	36	5	RTL	723	117	NA

LTL : left temporal lobe epilepsy, RTL : right temporal lobe epilepsy. Sl : asleep, Aw: awake.

APPENDIX B

NETWORK PARAMETERS

B.1. Louvain algorithm for community assignment

The BCT function for community assignment uses the Louvain community detection algorithm [32] with modularity maximization [50, 51] using an iterative process.

The community detection algorithm with modularity maximization aims to maximize the modularity quality statistic Q ,

$$Q = \sum_{i,j} [S_{i,j} - \gamma P_{ij}] \delta(g_i, g_j) \quad (\text{B.1})$$

Where S is the network's adjacency matrix, g_i is the community assigned to node i and g_j is the community assigned to node j . $\delta(g_i, g_j) = 1$ if the community assignments $g_i = g_j$ and 0 otherwise. $P_{i,j}$ is the expected weight of the edge between i and j under a specific null model. The resolution parameter γ modifies the weights of $P_{i,j}$. Here we use the Newman-Girvan null model of the form

$$P_{i,j} = \frac{k_i k_j}{2m}, \quad (\text{B.2})$$

where $k_i = \sum_j S_{i,j}$ and $m = \frac{1}{2} \sum_{i,j} S_{i,j}$.

APPENDIX C

SUMPLEMENTARY FIGURES : COMMUNITY DETECTION AND ANALYSIS

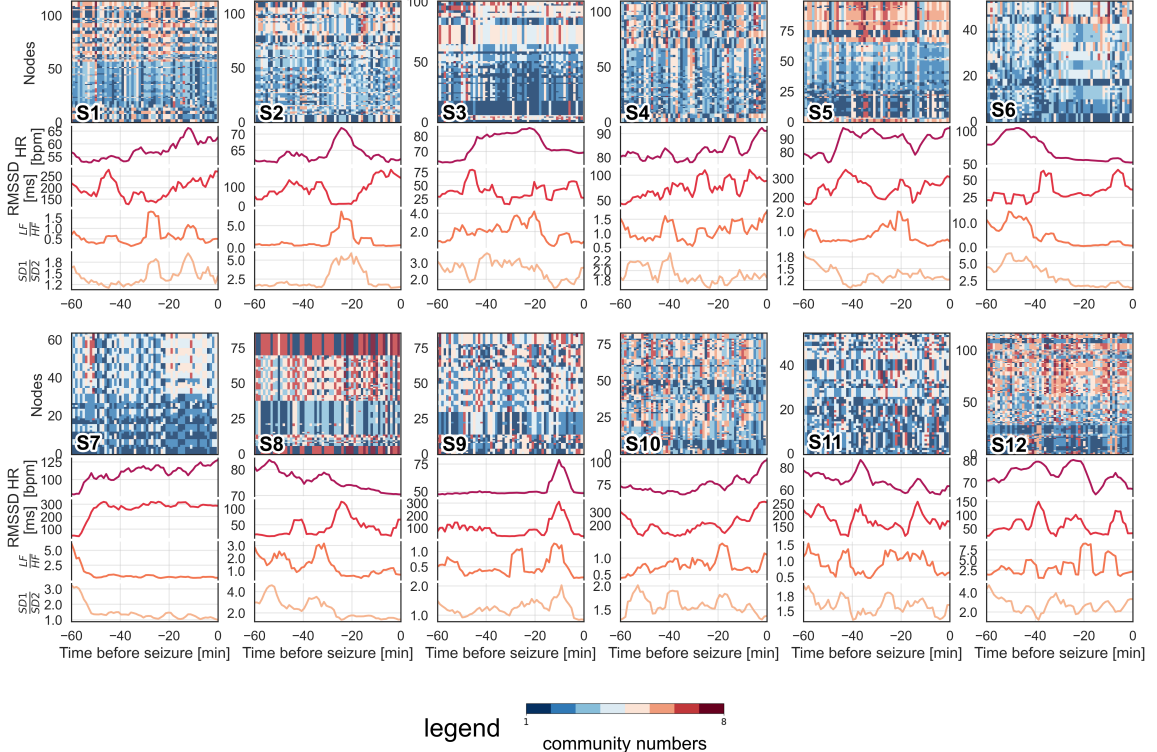


Figure C.1: Node-wise core-periphery grouping changes and HRV parameters over time windows. The plot shows the data from each of the 12 subjects. For each 1-min window, a functional network was built using Pearson r values (edges) between electrode pairs (nodes). For each network (window) the nodes were assigned communities based on the Louvain algorithm. The community assignments with a median value of modularity after 100 iterations of the algorithm were selected. The bottom plots show the HR parameters, HR, RMSSD, LF/HF and SD1/SD2 calculated from the ECG signal in a 1-min window.

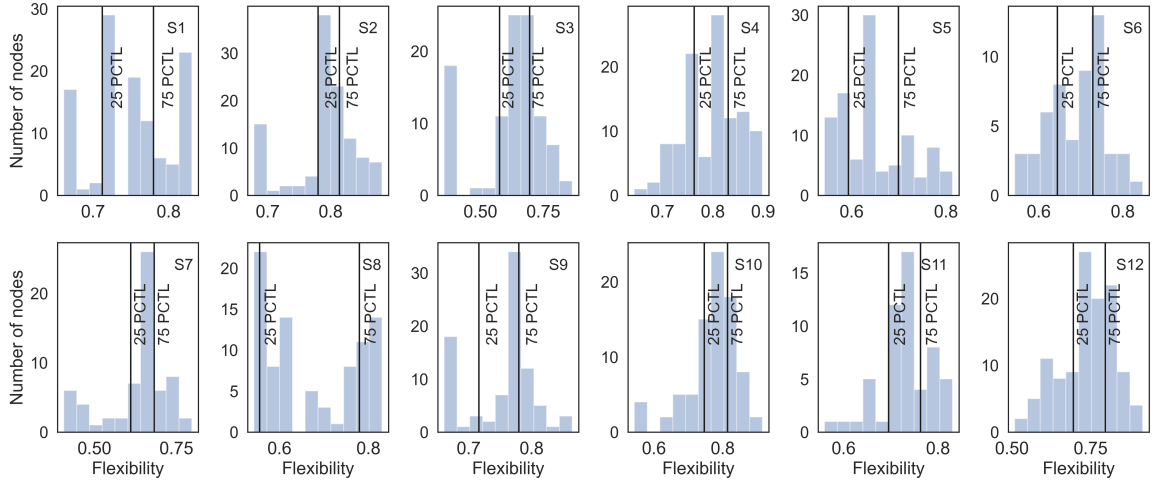


Figure C.2: Flexibility distribution of core-periphery group changes of network nodes. The plot shows flexibility distribution for all 12 subjects. Flexibility indicates the number of community assignment changes of each node across time windows, normalized by the total number of possible changes. Based on the flexibility (F) values, the nodes were divided into 3 clusters, $F \leq 25$ PCTL, $25 < F \leq 75$ PCTL and $F > 75$ PCTL. These thresholds have been marked on the plots.

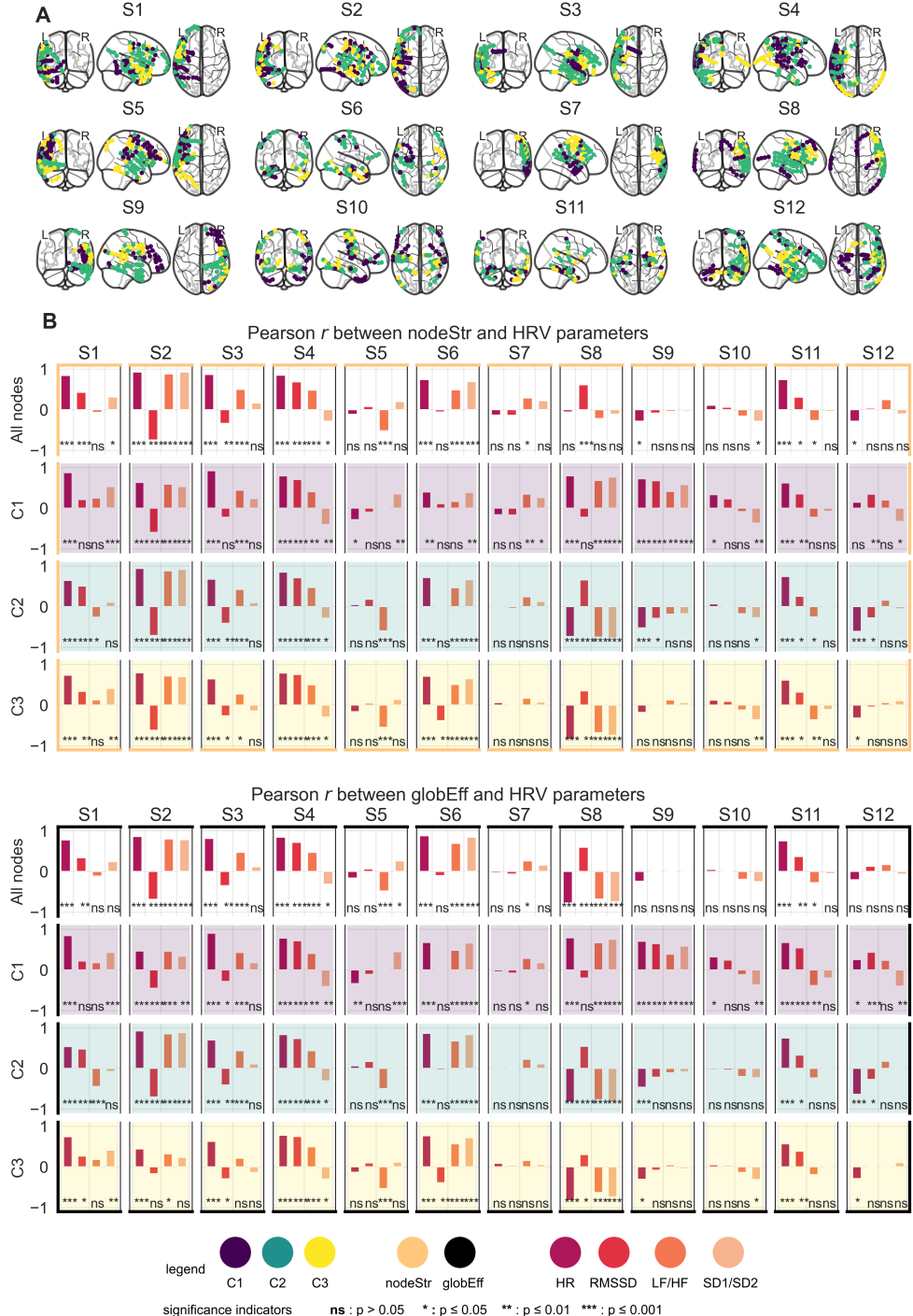


Figure C.3: Correlation of HRV parameters with network parameter of all nodes and clustered nodes : The plots show data from all 12 subjects. **A** The location of all the nodes for each subject along with the cluster groupings based on flexibility are shown. **B** The two groups of plots show the correlations between HRV parameters and the two network properties. The top plots show the r values with nodeStr for all nodes, C1, C2 and C3 node clusters. Similarly, the bottom plots show the r values with globEff. For each bar a significant indicator is marked at the bottom. The degree of freedom for all r values is 58.

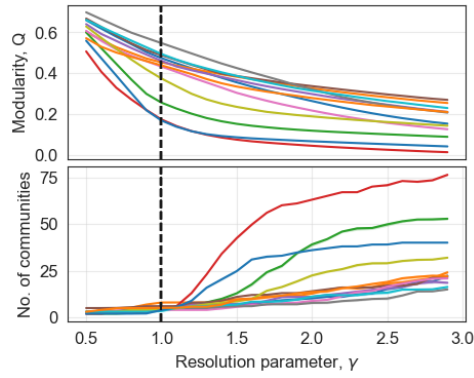


Figure C.4: Selection of optimal γ The plot shows the use of Louvain algorithm and changes in the Q value and number of communities for variations in γ for 0.5 to 3, with 100 iterations performed at each value. Each line represents a single subject and an adjacency matrix from one window. The solid line is the mean value and the shaded region represents 1 standard deviation about the mean from the 100 iterations. A $\gamma = 1$ provided the optimal size of communities across all subjects.

BIBLIOGRAPHY

- [1] EFEPA - Epilepsy Foundation Eastern Pennsylvania (2021) Types of seizures (<https://www.efepa.org/living-with-epilepsy/types-of-seizures/>). [Online; accessed 04-25-2022].
- [2] Liu G, Associates HVM (2017) Epilepsy: Treatment Options. 96(2):10.
- [3] Shorvon S (2010) *Handbook of Epilepsy Treatment*. (John Wiley & Sons). Google-Books-ID: ce1YGxllLsgC.
- [4] EFEPA - Epilepsy Foundation Eastern Pennsylvania (2019) Living with epilepsy (<https://www.efepa.org/living-with-epilepsy/>). [Online; accessed 04-25-2022].
- [5] EFEPA - Epilepsy Foundation Eastern Pennsylvania (2021) Treatment options (<https://www.efepa.org/living-with-epilepsy/#LWE3>). [Online; accessed 04-25-2022].
- [6] Rho JM, White HS (2018) Brief history of anti-seizure drug development. *Epilepsia Open* 3(Suppl Suppl 2):114–119.
- [7] Fisher RS, et al. (2000) The impact of epilepsy from the patient's perspective II: views about therapy and health care. *Epilepsy Research* 41(1):53–62.
- [8] Balamurugan E, Aggarwal M, Lamba A, Dang N, Tripathi M (2013) Perceived trigger factors of seizures in persons with epilepsy. *Seizure* 22(9):743–747.
- [9] Ge A, et al. (2022) Seizure triggers identified postictally using a smart watch reporting system. *Epilepsy & Behavior* 126:108472.
- [10] Novakova B, Harris PR, Ponnusamy A, Reuber M (2013) The role of stress as a trigger for epileptic seizures: A narrative review of evidence from human and animal studies. *Epilepsia* 54(11):1866–1876. _eprint: <https://onlinelibrary.wiley.com/doi/pdf/10.1111/epi.12377>.
- [11] Cohen S, ed. (1997) *Measuring stress: a guide for health and social scientists*, A project of the Fetzer Institute. (Oxford University Press, New York).
- [12] Devinsky O (2004) Effects of Seizures on Autonomic and Cardiovascular Function. *Epilepsy Currents* 4(2):43–46.
- [13] Whitney R, Donner EJ (2019) Risk Factors for Sudden Unexpected Death in Epilepsy (SUDEP) and Their Mitigation. *Current Treatment Options in Neurology* 21(2):7.
- [14] Eggleston KS, Olin BD, Fisher RS (2014) Ictal tachycardia: The head–heart connection. *Seizure - European Journal of Epilepsy* 23(7):496–505. Publisher: Elsevier.
- [15] Yilmaz M, Kayancicek H, Cekici Y (2018) Heart rate variability: Highlights from hidden signals. *Journal of Integrative Cardiology* 4(5).

- [16] Wikipedia contributors (2022) Wearable technology — Wikipedia, the free encyclopedia (https://en.wikipedia.org/w/index.php?title=Wearable_technology&oldid=1084977924). [Online; accessed 04-25-2022].
- [17] Brinkmann BH, et al. (2021) Seizure Diaries and Forecasting With Wearables: Epilepsy Monitoring Outside the Clinic. *Frontiers in Neurology* 12.
- [18] Regalia G, Onorati F, Lai M, Caborni C, Picard RW (2019) Multimodal wrist-worn devices for seizure detection and advancing research: Focus on the Empatica wristbands. *Epilepsy Research* 153:79–82.
- [19] Stone JD, et al. (2021) Assessing the Accuracy of Popular Commercial Technologies That Measure Resting Heart Rate and Heart Rate Variability. *Frontiers in Sports and Active Living* 3.
- [20] Hernando D, Roca S, Sancho J, Alesanco Bailón R (2018) Validation of the Apple Watch for Heart Rate Variability Measurements during Relax and Mental Stress in Healthy Subjects. *Sensors (Basel, Switzerland)* 18(8):2619.
- [21] Shaffer F, Ginsberg JP (2017) An Overview of Heart Rate Variability Metrics and Norms. *Frontiers in Public Health* 5:258.
- [22] Malik M, et al. (1996) Heart rate variability: Standards of measurement, physiological interpretation, and clinical use. *European Heart Journal* 17(3):354–381.
- [23] Jeppesen J, Beniczky S, Johansen P, Sidenius P, Fuglsang-Frederiksen A (2014) Using Lorenz plot and Cardiac Sympathetic Index of heart rate variability for detecting seizures for patients with epilepsy in *2014 36th Annual International Conference of the IEEE Engineering in Medicine and Biology Society*. pp. 4563–4566. ISSN: 1558-4615.
- [24] Delamont RS, Walker MC (2011) Pre-ictal autonomic changes. *Epilepsy Research* 97(3):267–272.
- [25] Kassinopoulos M, Harper RM, Guye M, Lemieux L, Diehl B (2021) Altered Relationship Between Heart Rate Variability and fMRI-Based Functional Connectivity in People With Epilepsy. *Frontiers in Neurology* 12:953.
- [26] de la Cruz F, et al. (2019) The relationship between heart rate and functional connectivity of brain regions involved in autonomic control. *NeuroImage* 196:318–328.
- [27] Wagenaar JB, Brinkmann BH, Ives Z, Worrell GA, Litt B (2013) A multimodal platform for cloud-based collaborative research in *2013 6th International IEEE/EMBS Conference on Neural Engineering (NER)*. pp. 1386–1389. ISSN: 1948-3554.
- [28] Rubinov M, Sporns O (2010) Complex network measures of brain connectivity: Uses and interpretations. *NeuroImage* 52(3):1059–1069.

- [29] Carreiras C, et al. (2015–) BioSPPy: Biosignal processing in Python (<https://github.com/PIA-Group/BioSPPy/>). [Online; accessed 04-25-2022].
- [30] Gomes P, Margaritoff P, Silva H (2019) pyHRV: Development and evaluation of an open-source python toolbox for heart rate variability (HRV) in *Proc. Int'l Conf. on Electrical, Electronic and Computing Engineering (IcETRAN)*. pp. 822–828.
- [31] Nussinovitch U, et al. (2011) Reliability of Ultra-Short ECG Indices for Heart Rate Variability. *Annals of Noninvasive Electrocardiology: The Official Journal of the International Society for Holter and Noninvasive Electrocardiology, Inc* 16(2):117–122.
- [32] Blondel VD, Guillaume JL, Lambiotte R, Lefebvre E (2008) Fast unfolding of communities in large networks. *Journal of Statistical Mechanics: Theory and Experiment* 2008(10):P10008. arXiv: 0803.0476.
- [33] Telesford QK, et al. (2016) Detection of functional brain network reconfiguration during task-driven cognitive states. *NeuroImage* 142:198–210.
- [34] Bassett DS, et al. (2011) Dynamic reconfiguration of human brain networks during learning. *Proceedings of the National Academy of Sciences of the United States of America* 108(18):7641–7646.
- [35] Courten S, et al. (2016) Graph Measures of Node Strength for Characterizing Preictal Synchrony in Partial Epilepsy. *Brain Connectivity* 6(7):530–539. Publisher: Mary Ann Liebert, Inc., publishers.
- [36] Hödl S, et al. (2021) Pre-ictal heart rate variability alterations in focal onset seizures and response to vagus nerve stimulation. *Seizure* 86:175–180.
- [37] Behbahani S, Dabanloo NJ, Nasrabadi AM, Teixeira CA, Dourado A (2013) Pre-ictal heart rate variability assessment of epileptic seizures by means of linear and non-linear analyses. *Anadolu Kardiyoloji Dergisi/The Anatolian Journal of Cardiology*.
- [38] Dono F, et al. (2020) Interictal Heart Rate Variability Analysis Reveals Lateralization of Cardiac Autonomic Control in Temporal Lobe Epilepsy. *Frontiers in Neurology* 11:842.
- [39] Chang C, et al. (2013) Association between heart rate variability and fluctuations in resting-state functional connectivity. *NeuroImage* 68:93–104.
- [40] Alba G, Vila J, Rey B, Montoya P, Muñoz M2019) The Relationship Between Heart Rate Variability and Electroencephalography Functional Connectivity Variability Is Associated With Cognitive Flexibility. *Frontiers in Human Neuroscience* 13:64.
- [41] Napadow V, et al. (2008) Brain correlates of autonomic modulation: Combining heart rate variability with fMRI. *NeuroImage* 42(1):169–177.
- [42] Bernd Thomas (2017–) Sensorlog v5.2 (<http://sensorlog.berndthomas.net/>). [Online; accessed 04-25-2022].

- [43] Koester M (2021) Quantified Self Personal Data Aggregator and Data Analysis (https://github.com/markwk/qs_ledger/). [Online; accessed 04-25-2022].
- [44] Bland JM, Altman DG (2010) Statistical methods for assessing agreement between two methods of clinical measurement. *International Journal of Nursing Studies* p. 6.
- [45] Myles PS, Cui J (2007) I. Using the Bland–Altman method to measure agreement with repeated measures. *BJA: British Journal of Anaesthesia* 99(3):309–311.
- [46] Minarini G (2020) *Root Mean Square of the Successive Differences as Marker of the Parasympathetic System and Difference in the Outcome after ANS Stimulation*. (In-techOpen). Publication Title: Autonomic Nervous System Monitoring - Heart Rate Variability.
- [47] DeGiorgio CM, et al. (2010) RMSSD, a measure of vagus-mediated heart rate variability, is associated with risk factors for SUDEP: The SUDEP-7 Inventory. *Epilepsy & Behavior* 19(1):78–81.
- [48] Altini M, Amft O (2016) HRV4Training: Large-scale longitudinal training load analysis in unconstrained free-living settings using a smartphone application in *2016 38th Annual International Conference of the IEEE Engineering in Medicine and Biology Society (EMBC)*. pp. 2610–2613. ISSN: 1558-4615.
- [49] Romigi A, et al. (2016) Heart rate variability in untreated newly diagnosed temporal lobe epilepsy: Evidence for ictal sympathetic dysregulation. *Epilepsia* 57(3):418–426. _eprint: <https://onlinelibrary.wiley.com/doi/10.1111/epi.13309>.
- [50] Mucha PJ, Richardson T, Macon K, Porter MA, Onnela JP (2010) Community Structure in Time-Dependent, Multiscale, and Multiplex Networks. *Science* 328(5980):876–878. arXiv: 0911.1824.
- [51] Scheid BH, et al. (2021) Time-evolving controllability of effective connectivity networks during seizure progression. *Proceedings of the National Academy of Sciences of the United States of America* 118(5):e2006436118.